Constraints on the Origin of the ca 1780 Ma High Heat Producing Napperby Gneiss, Aileron Province, Central Australia

Thesis submitted in accordance with the requirements of the University of Adelaide for an Honours Degree in Geology

Samuel Weiss

November 2016

THE UNIVERSITY of ADELAIDE

CONSTRANINTS ON THE ORIGIN OF THE CA 1780 MA HIGH HEAT PRODUCING NAPPERBY GNEISS, AILERON PROVINCE, CENTRAL AUSTRALIA

ORIGIN OF THE NAPPERBY GNEISS

ABSTRACT

The Arunta Region of Central Australia contains Paleoproterozoic granites extremely enriched in high heat producing elements, in comparison to a global upper crustal average of 1.69 μWm^{-3}. This study uses geochemistry, geochronology, and zircon saturation thermometry to investigate the source and tectonic environment of emplacement of the ca. 1780 Ma Napperby Gneiss.
The Napperby Gneiss is peraluminous, suggesting a metasedimentary source. Samples have negative Eu anomalies ranging from 0.10 to 0.57, and show further evidence of fractionation in negative correlations of Ba and Sr with increasing SiO_2
Initial εNd values are similar to surrounding exposed metasedimentary rocks and suggest a strong influence of an evolved crustal source but indicate a necessary juvenile component.
Matches of inherited xenocrystic zircons from the gneiss with detrital patterns from the regional metasedimentary Lander Formation indicate that sediments similar to the Lander Formation are the source of the protolith granite. Zircon saturation temperatures suggest the granites were emplaced at 790°C – 872°C. Heat production is less than the slightly older ca 1800 ma suites of the Aileron province, and zircon saturation temperatures are higher. The Napperby was produced by dehydration melting rather than fluid flux melting, possibly in a back arc extensional environment with heat provided by upwelling mantle.

KEYWORDS

High Heat Producing, Geochemistry, Central Australia, zircon saturation thermometry, Reynolds Ranges, Arunta Complex, Aileron Province, Napperby Gneiss

TABLE OF CONTENTS

LIST OF FIGURES AND TABLES

1 INTRODUCTION

The major influences on the availability of elements within a magmatic system are the composition of the source, degree of partial melting, and degree of differentiation during the ascent and emplacement of the magma body. Bea (2012) states that the composition of the source is the main factor controlling whether a granite will be high-heat producing; moreover, that metasedimentary rocks are more likely to produce high heat producing (HHP) granitoides compared to metabasic rocks due to higher concentrations of U, Th, and K in metasedimentary rocks. Bea (2012) goes on to conclude that sources already enriched in heat-producing elements (HPE) are more likely to produce HHP granitoides.

The Proterozoic crustal rocks of central Australia have been shown to have significantly elevated concentrations of Uranium and Thorium compared to the global average of Proterozoic crust (Hand and Buick 2001, McLaren et al. 2005), leading to the classification of a significant number of Proterozoic Australian terranes HHP. These HHP rocks, especially those from the North Australian Craton, exhibit elevated heat flows due to this enrichment in the highly radioactive elements compared to rocks of similar age in other localities (Figure 1). The igneous rocks of the Australian Proterozoic are important for understanding the interaction between the crust and the mantle during the generation of HHP granitic magma. The generation of such magmas can strongly differentiate crustal material, which will result in concentration of highly incompatible HPE, such as Uranium and Thorium (Taylor and McLennan 1985, Wark and Miller 1993, Kemp et al. 2007, Hawkesworth et al. 2010, Bea, 2012).

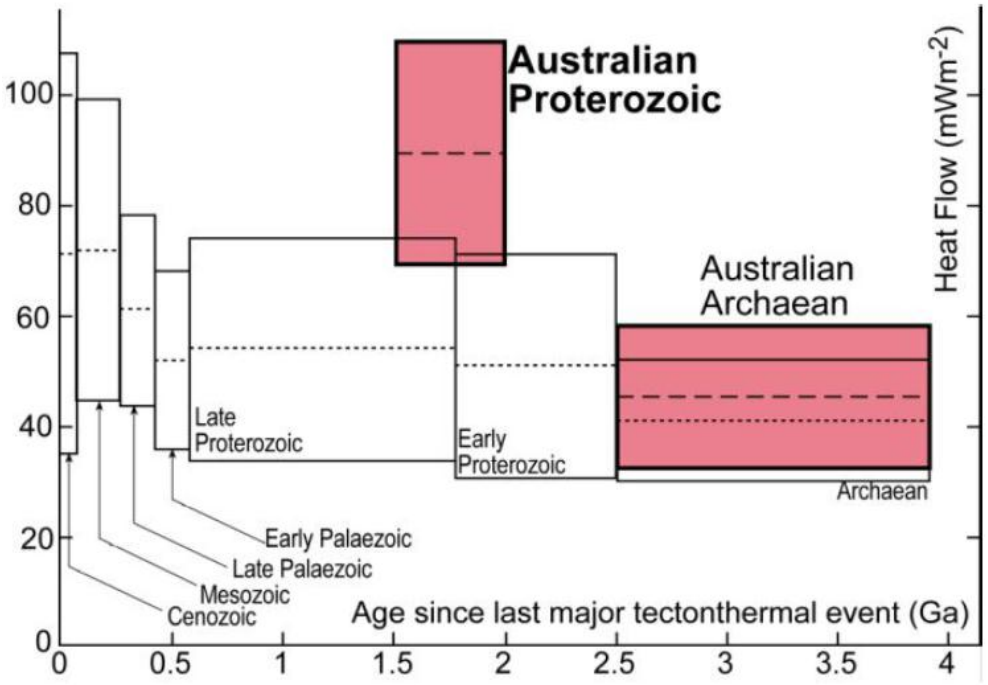

Figure 1: Histogram of global modern continental surface heat flow data (McLaren et al., 2003).

Sandiford et al. (2002) put forth that the HHP granites of the Australian Proterozoic were sourced from the melting of a deep crustal source by addition from the asthenosphere, with the mantle material possibly serving as source material and/or a thermal source for the melting of lower crust material. McLaren et al. (2005) suggest that crustal reworking via partial melting, along with mixing of crustal and mantle melts, was the cause of enrichment in HPEs in the HHP granites. McLaren & Powell (2014) looked at the HHP granites of the North Australian craton and proposed a 'hot-plate' orogenic style model. Their model proposes that the orogenic styles involved minimal crustal thickening, with additions from a more juvenile magma. McLaren & Powell (2014) conclude that the addition of HPE from juvenile mantle material into a preferentially enriched crustal system helps to account for the higher average heat production in younger granites of the Proterozoic North Australian Craton.

This study focuses on the Napperby Gneiss (1780 ± 10 Ma; Collins and Williams, 1995; Reid, 2012), a ca. 200,000 km^2 peraluminous unit found within the southern Reynolds and Yalyirimbi ranges of the southern Arunta Complex (Figure 3). Previous work on the Napperby Gneiss by Stewart et al. (1980) mention the presence of calc-silicate xenoliths along the northern margin of the Napperby,

which they concluded to be a unit of the Reynolds Range Group. Reid (2012) sampled a metasedimentary raft within the Napperby that they believed had an age signature similar to that of the Lander Formation.

This project aims to investigate how mantle derived material and intracontinental recycling relate to the development of the Napperby Gneiss in the Aileron Province, identify the potential source rock, and explain the high heat producing nature of this unit.

U-Pb geochronology of inherited zircon xenocrysts will be collected for the Napperby Gneiss and for the metasedimentary raft previously looked at by Reid (2012). These data will be compared with the detrital zircon populations of exposed metasedimentary rocks of the Aileron Province to characterise the source region that produced the granites. Geochemical and εNd isotope data will be used to determine the extent of influence that the crust and the mantle had on development of the granitic predecessor to the Napperby Gneiss. Results from this study have significance in supplementing our knowledge of how Proterozoic Australia became so extraordinarily enriched in HPEs.

2 GEOLOGICAL SETTING

The Arunta Complex, located in central Australia, defines the southern portion of the North Australian Craton (NAC; Figure 2). It is believed to have a significant role in the assembly and growth of the Australian continent in the Proterozoic (Wade et al 2006). A number (at least six) tectonic events are recorded over an extended period from ca. 1860 Ma to ca. 1550 Ma (Hand & Buick 2001, Betts & Giles 2006, Claoue-Long et al. 2008). The prevalent view is that the southern margin of the NAC represents a long-lived (ca. 300 Myr) active margin in many large-scale tectonic models (Scrimgeour et al. 2005, Betts & Giles 2006, Cawood & Korch 2008).

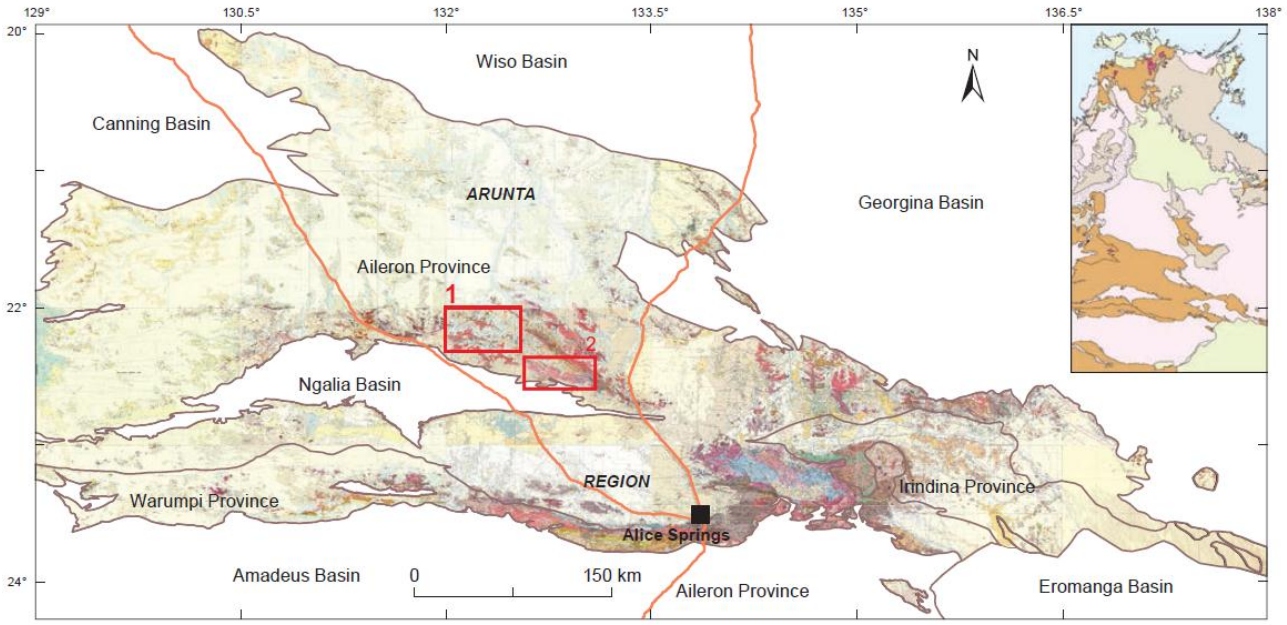

Figure 2: Schematic regional geological map of the Arunta Region showing (1) Wangala Granite and (2) Napperby Gneiss, with inset showing position within the Northern Territory. Modified from Beyer et al. 2012.

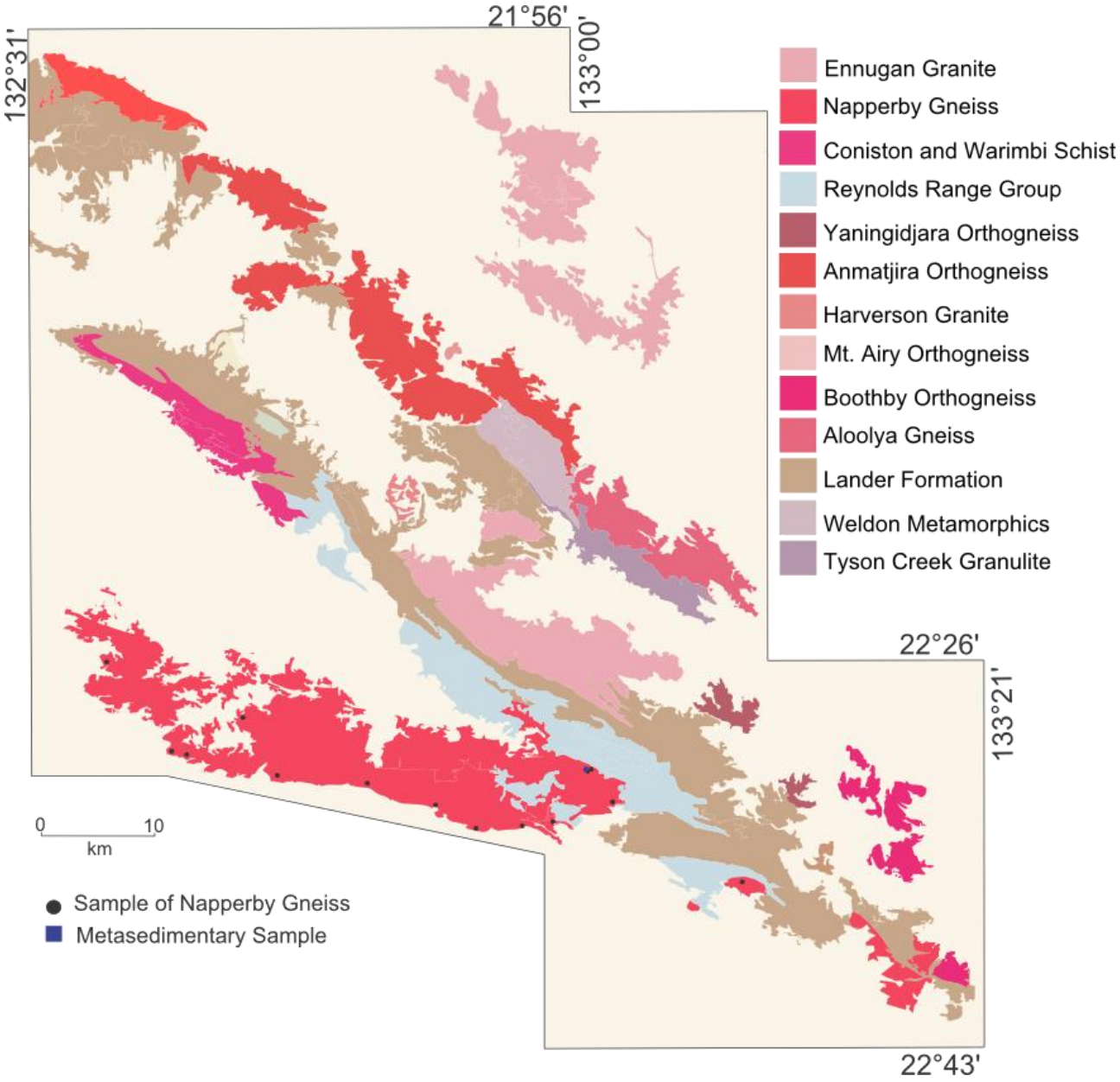

Figure 3: Map showing sample locations throughout the Reynold Ranges, modified from Stewart et al.

The Arunta Complex encompasses an approximate 200,000 km^2 region of Paleoproterozoic to Palaeozoic aged (Shaw et al., 1984), intermediate to high grade metamorphic rocks, juxtaposed against sedimentary basins of Neoproterozoic to Phanerozoic ages (Collins and Shaw, 1995). The history of the Arunta Complex is complex with periods of extension, represented as sedimentary basins that are punctuated by periods of magmatism and/or metamorphism (Hand & Buick 2001). The Arunta Complex is generally subdivided into three distinct provinces (Fig. 2) marked by differing protolith ages and histories (Scrimgeour *et al.* 2005):

1) The Aileron Province, which is the largest of the three provinces, contains rocks with depositional and intrusive ages between 1870–1710 Ma (Scrimgeour *et al.* 2005, Claoue-Long *et al.* 2008);
2) The Warumpi Province, which occurs on the southern margin on the Arunta Complex, has intrusive and sediment protolith ages between *ca*. 1690–1600 Ma (Scrimgeour *et al.* 2005). Scrimgeour et al. (2005) propose that the Warumpi Province is an exotic terrane;
3) The Irindina Province, located in the south-eastern Arunta Complex, contains sedimentary and igneous protoliths ranging from Neoproterozoic to Cambrian in age (Buick *et al.* 2001).

The tectonic history of the Arunta Complex has multiple tectonothermal cycles spanning ca. 1820 Ma - 300 Ma. In the Palaeoproterozic these include the ca. 1820-1800 Ma Stafford Event which consisted of bimodal magmatism and low-pressure high-temperature metamorphism (Collins & Vernon 1991). The ca. 1790-1770 Ma early Strangways Orogeny, also called the Yambah Event, which resulted in voluminous magmatism throughout the Arunta region associated with various degrees of deformation and metamorphism, with contact metamorphism present around the granitic precursors to the Coniston and Warimbi schists that intruded the Reynolds Range Group around 1785 (Collins & Williams 1995, Hand & Buick 2001). These two events are responsible for widespread greenschist to granulite facies metamorphism and are associated with the emplacement of granites throughout the Reynolds-Anmatjira-Yalyirimbi Ranges (Hand and Buick 2001), including the precursor of the Napperby Gneiss. The ca. 1760-1740 Ma Inkamulla Igneous Event (Scrimgeour 2003) was an episode of voluminous granitic and minor mafic magmatism throughout the southern and eastern Arunta region. Dirks et al (1991) place this event as the age of emplacement of granites in the Reynolds Ranges, with no known associated metamorphism. The ca. 1730-1690 Ma Strangways Orogeny was a major tectonic event, resulting in extensive deformation and metamorphism in the Arunta region (Hand & Buick 2001, Scrimgeour 2003). The ca. 1669-1630 Liebig Orogeny in the Warumpi Province has been interpreted as the accretion of the province onto the NAC (Scrimgeour 2003). The ca. 1590-1560 Chewings Orogeny has shown variable impact across the Arunta region, resulting in a transition in metamorphic grade from greenschist to granulite

facies within the Reynolds Ranges (Vry et al., 1996; Hand & Buick, 2001), and the intrusion of pegmatite dykes in the Reynolds-Anmatjira ranges (Collins & Williams, 1995). The Palaeozoic ca. 400 -300 Ma Alice Springs Orogeny was a long-lived and episodic event which resulted in the exhumation of the Arunta region (Cartwright et al., 1999).

2.2 Reynolds Ranges:

The Reynolds-Anmatjira-Yalyirimbi Ranges (Fig. 2) within the Aileron Province trend approximately 130 km in a NW-SE direction. Within the Reynolds-Anmatjira-Yalyirimbi Ranges there are four rock 'packages' that have been distinguished on the basis of unconformable and intrusive relationships (Dirks & Wilson, 1990). The oldest rock package in the area (and in the Arunta Region) is the Lander Formation, a sequence of sandstone and siltstones (Vry et al. 1996, Hand & Buick 2001, Claoue-Long et al. 2008, Scrimgeour 2013) deposited at ca. 1840–1830 Ma based on detrital zircon U-Pb ages obtained by Claoue-Long et al. (2008), with an equivalent package in the Stafford Beds (Scrimgeour 2013). The second 'package' is a series a granitic intrusions into the Lander Package at 1820 - 1790 Ma (Scrimgeour, 2013). The third 'package' is the Reynolds Range Group of sedimentary rocks which unconformably overlies the first two packages and is estimated to have been deposited in the interval ca. 1812–1785 Ma (Collins & Williams 1995, Hand & Buick 2001). The Reynolds Range Group comprises a basal quartzite unit overlain by interlayered units of pelites, quartzites, and calc-silicates (Dirks & Wilson 1990). The youngest 'package' is another series of granitic intrusions that includes the Napperby Gneiss. The age of this extensive magmatic rock system has been constrained from the Napperby Gneiss, by U-Pb zircon geochronology at ca. 1780 Ma (Collins & Williams 1995, Reid 2012). The Napperby Gneiss is reported to contain a complex and poorly understood geochronological record, and ages corresponding to the Yambah (Early Strangway), Inkamulla, Strangways and Liebig events have been reported from the Napperby Gneiss (Dirks & Hand 1991, Collins & Williams 1995). Along the northern margin of the Napperby Gneiss, calc-silicate xenoliths have been observed, and attributed to the Reynolds Range Group (Stewart et

al., 1980; Collins and Williams, 1995). Reid (2012) sampled a metasedimentary raft within the Napperby that when constrained by Th/U ratios gave a depositional age that suggested that the metasedimentary raft belonged in the Reynolds Range Group, however it was noted that the youngest detrital zircons had ages within analytical uncertainty of the minimum depositional age of the Lander Formation.

3 METHODS

Samples were prepared, from archived material, for analysis by cutting, crushing with a jaw crusher, and finally milling with a tungsten carbide millhead in the case of geochemical analysis or with a disk mill in the case of geochronological analysis.

Small rock slabs were sent to Continental Instruments, India to be processed into thin sections. The returned thin sections were petrologically interpreted by optical microscope.

Samples were prepared for external geochemical analysis by rock saw, crushing and milling, as outlined above. The samples were sent to Australian Laboratory Services Pty. Ltd. for whole rock, REE and trace element analysis. Returned data was manipulated using GCDkit.

U-Pb geochronology was undertaken at Adelaide Microscopy of the University of Adelaide. Analytical techniques of the zircons follow that of Payne et al. (2006). Using the SEM Quanta 66 MLA, zircon mounts were subjected to backscattered electron (BSE) and cathodoluminescence (CL) imaging to detect zonation within the zircon grains. U-Pb isotopic analyses were collected using a New Wave 213 nm Nd-YAG laser in a helium ablation atmosphere, coupled to an Agilent 7500cs/7500s ICP-MS. U-Pb fractionation is corrected using the GJ standard, with accuracy of the standard and machine drift is checked with the PLES standard (Plesovice zircon standard (Sláma et al. 2008)). Pb/Pb grain ages are used. Data was processed with the ‘IOLITE’ program (Chew et al 2014)

4 OBSERVATIONS AND RESULTS

4.1 Petrography

Seventeen samples of Napperby Gneiss were processed into thin sections (Appendix A).

In thin section (Figure 4) all samples contained biotite, quartz, plagioclase, and potassium feldspar, often in form of perthite and microcline. Cordierite and muscovite were also observed in small quantities in some samples.

When plotted on a Total Alkali Silica diagram following Middlemost (1994), samples from the Napperby Gneiss fall in the granitic field (Figure 5). The geochronologically equivalent Wangala granite from Mount Denison (ca. 1775 Ma; Beyer, 2012), and the slightly older (ca. 1800 Ma; Worden et al. 2008) but proximal Anmatjira Orthogneiss are shown for comparison.

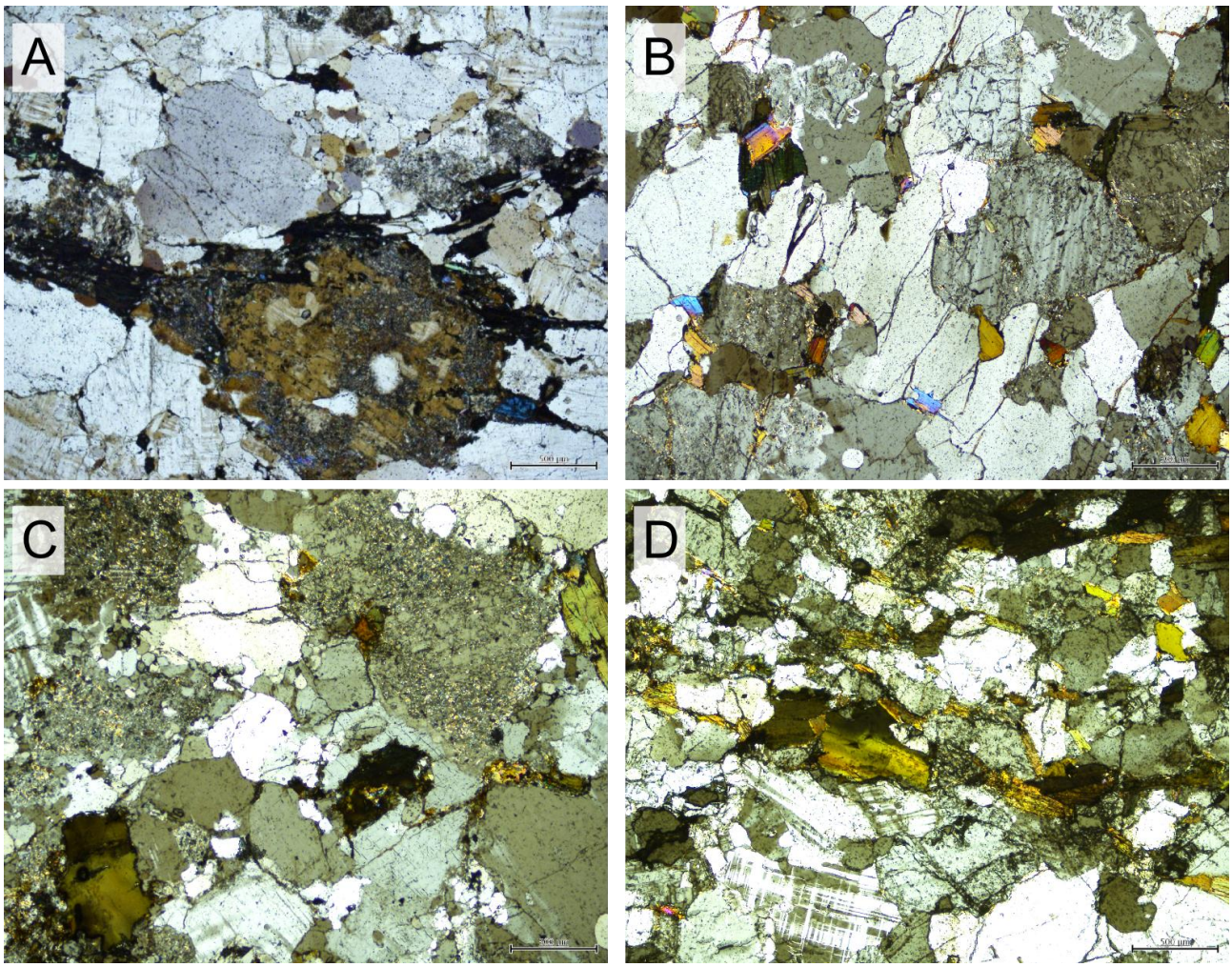

Figure 4: Representative photo micrographs of Napperby Gneiss. Bi= biotite, qz=quartz, plg= plagioclase, ksp=orthoclase, cd= cordierite, mu=muscovite

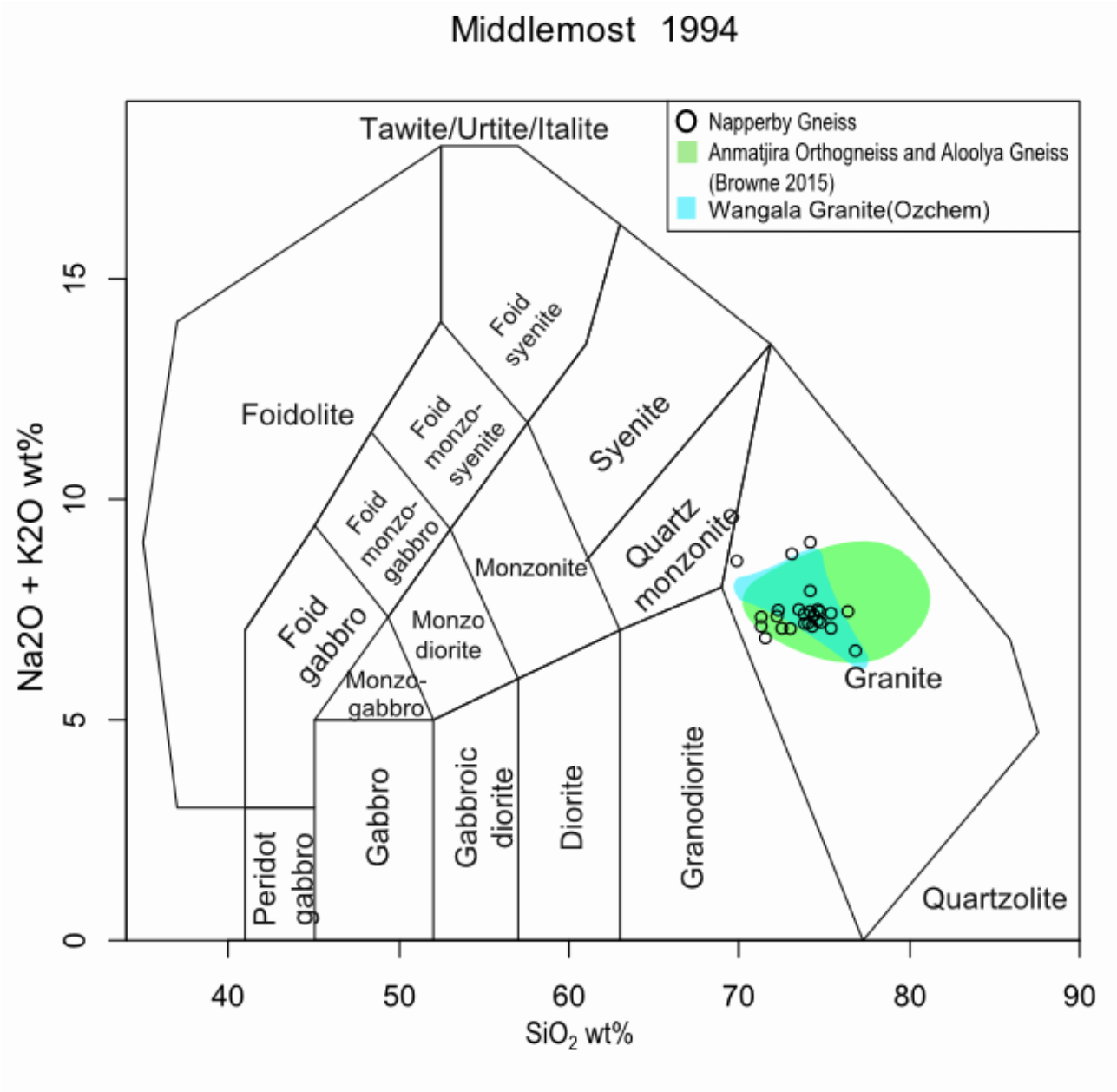

Figure 5: Total Alkali Silica diagram after Middlemost (1994) with samples plotted as per key and fields showing similarities to granitic rocks from the Anmatjira Range (Browne 2015) and the Wangala granite (Ozchem).

4.2 Geochemistry

4.2.1 MAJOR ELEMENTS

Major element geochemical results for all samples can be seen in Table 1, and other minor and trace geochemical datasets can be found in Appendix 2

Harker Plots are displayed (Figure 6).

Additional data from Browne (2015) of granitoids in the region and the Wangala granite (OZCHEM) are shown as fields in a similar fashion to the TAS plot (Figure 5).

Al_2O_3, Fe_2O_3, and MgO all show negative trends as SiO_2 increases while CaO, P_2O_5, TiO_2, Na_2O and K_2O show a flat trend with increasing SiO_2.

The majority of samples are enriched in K and plot as peraluminous on the Alumina Saturation Index (Figure 7).

4.2.2 TRACE AND RARE EARTH ELEMENTS

Trace element geochemical results can be seen in Appendix 2

Trace element spiderplots and rare earth element diagrams normalised to primitive mantle (McDonough and Sun, 1995) and chondrite (Boynton, 1984) respectively are presented in Figure 8.

The trace element spiderplots plots shows general enrichment in Large Ion Lithophile elements such as Rb, K and Th, and negative anomalies for Nb, Ti, Ba, Sr and P.

The chondrite-normalized REE patterns are mostly quite uniform, and show enrichments in LREE relative to flattish HREEs.

Table 1: Major Element geochemical data presented with rock description and classification.

Sample ID	Suite Name	SiO_2	TiO_2	Al_2O_3	Fe_2O_3	MnO	MgO	CaO	Na_2O	K_2O	P_2O_5	Total	LOI
72921017	Napperby Gneiss	73.1	0.42	13.75	3.85	0.03	0.68	1.88	2.6	4.84	0.14	101.84	0.48
72921019	Napperby Gneiss	74.2	0.39	13.4	2.66	0.01	0.51	1.72	3.12	4.05	0.16	100.74	0.43
85924153	Napperby Gneiss	73	0.3	13.15	3.19	0.02	0.37	1.05	2.12	6.64	0.14	100.63	0.6
85924155	Napperby Gneiss	73	0.42	12.5	3.38	0.04	0.58	1.6	2.27	4.82	0.11	99.1	0.29
85924167	Napperby Gneiss	69.9	0.57	12.95	4.48	0.06	0.92	2.01	2.07	4.63	0.14	98.34	0.5
85924196	Napperby Gneiss	69.9	0.24	14.25	2.45	0.02	0.65	2.01	4.05	3.16	0.06	97.3	0.42
85924200	Napperby Gneiss	74.9	0.3	13.25	2.48	0.03	0.49	1.43	2.6	4.6	0.11	100.76	0.47
85924162C	Napperby Gneiss	73.7	0.39	13.1	3.05	0.03	0.49	1.62	2.2	5.17	0.15	100.43	0.42
85924163A	Napperby Gneiss	73.2	0.54	13.15	4.04	0.04	0.61	2.08	2.32	4.8	0.16	101.22	0.19
85924183A	Napperby Gneiss	73.8	0.48	12.9	4.22	0.04	0.64	1.72	2.4	4.75	0.17	101.55	0.33
NAP2010-11	Napperby	71	0.52	13.6	4.21	0.05	0.87	1.99	2.43	4.84	0.18	100.16	0.39
NAP2010-12	Napperby	68.7	0.52	13.3	4.14	0.05	0.79	1.83	2.3	4.56	0.21	97.09	0.6
NAP2010-2	Napperby	76.6	0.32	12.6	1.09	0.02	0.97	1.39	3.83	2.68	0.2	100.15	0.42
NAP2010-3	Napperby	74.2	0.31	13	2.02	0.02	0.47	1.08	3.25	4.02	0.12	99.19	0.62
NAP2010-4	Napperby	74.5	0.4	13.45	2.62	0.03	0.56	1.47	3.19	3.93	0.13	100.88	0.52
NAP2010-5	Napperby	72.8	0.17	13.5	1.63	0.02	0.24	0.88	2.12	6.73	0.09	98.85	0.62
NAP2010-6	Napperby	74.4	0.33	13.2	2.59	0.03	0.36	1.26	2.06	5.42	0.16	100.52	0.62
NAP2010-7	Napperby	72	0.35	12.45	2.82	0.03	0.41	1.38	2.15	4.85	0.15	97.22	0.54
NAP2010-8	Napperby	72.7	0.27	13.5	2.17	0.02	0.33	1.04	1.87	5.88	0.21	98.77	0.69
NAP2010-9	Napperby	68.1	0.28	16.3	2.32	0.03	0.36	1.56	2.6	5.77	0.19	98.44	0.85
NAP2012-10	Napperby	75.5	0.35	13.4	1.93	0.02	0.39	1.74	2.98	4.53	0.16	101.39	0.27
NAP2012-11a	Metasedimentary raft	59.3	0.75	18.75	7.91	0.05	2.72	0.42	1.12	3.64	0.05	95.57	0.75
NAP2012-12	Napperby	73.7	0.41	12.45	2.89	0.02	1.23	1.03	2.05	5.23	0.14	99.58	0.39
NAP2012-15	Napperby	74.9	0.33	12.95	2.23	0.02	0.37	1.42	2.45	4.55	0.12	99.82	0.38
NAP2012-4	Napperby	73.9	0.36	13.15	2.82	0.04	0.46	1.35	2.3	5.09	0.12	100.12	0.44
NAP2012-6	Napperby	71.6	0.39	13.15	3.15	0.02	0.6	1.11	2.3	4.98	0.16	98.39	0.83
NAP2012-8	Napperby	74.9	0.25	13	0.51	0.01	0.23	1.62	3.02	4.29	0.18	98.35	0.23

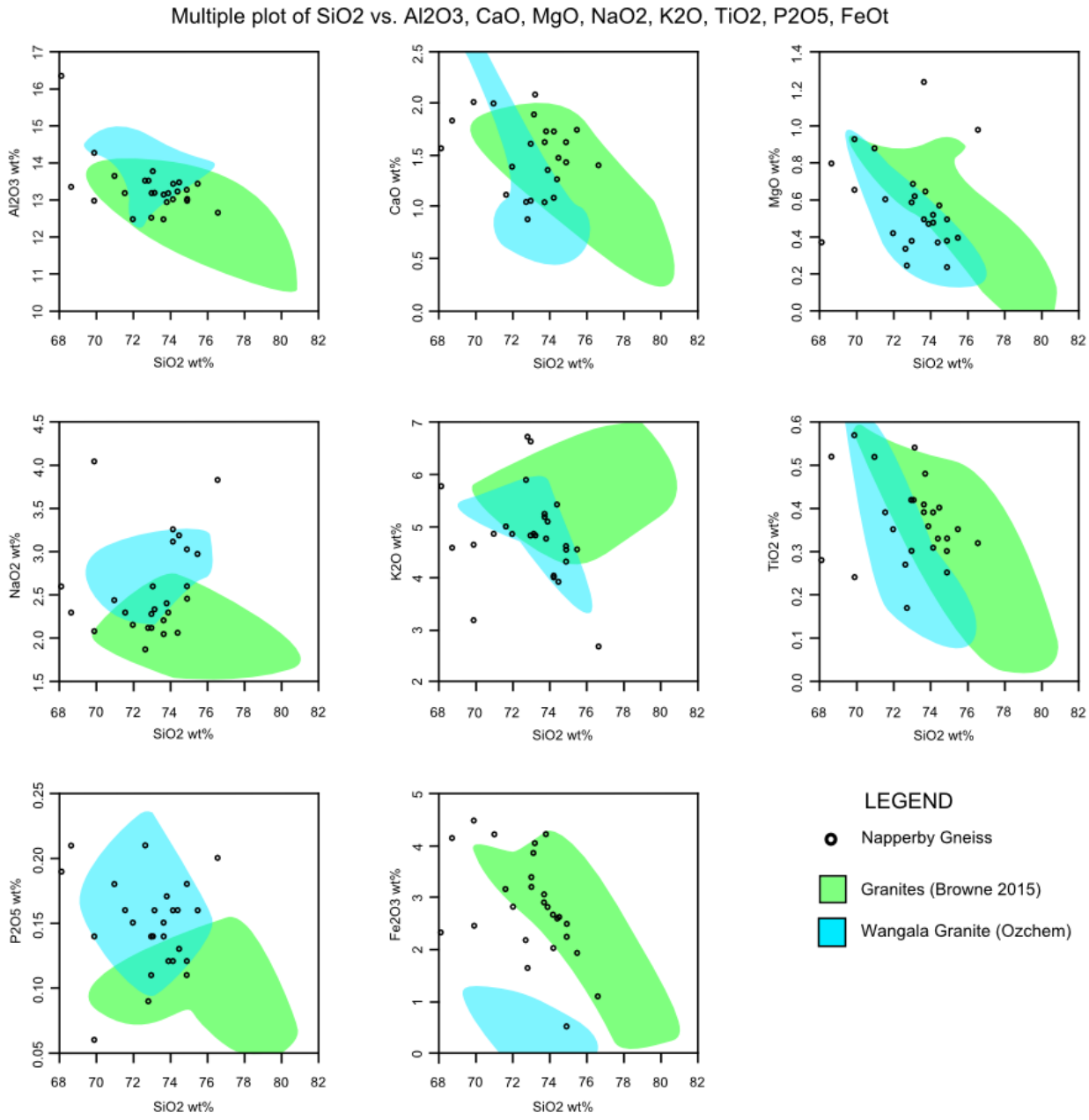

Figure 6: Harker Plots of SiO2 vs. major elements analysed with samples plotted as per legend and fields showing similarities to granitic rocks from the Anmatjira Range (Browne 2015) and the Wangala Granite (Ozchem).

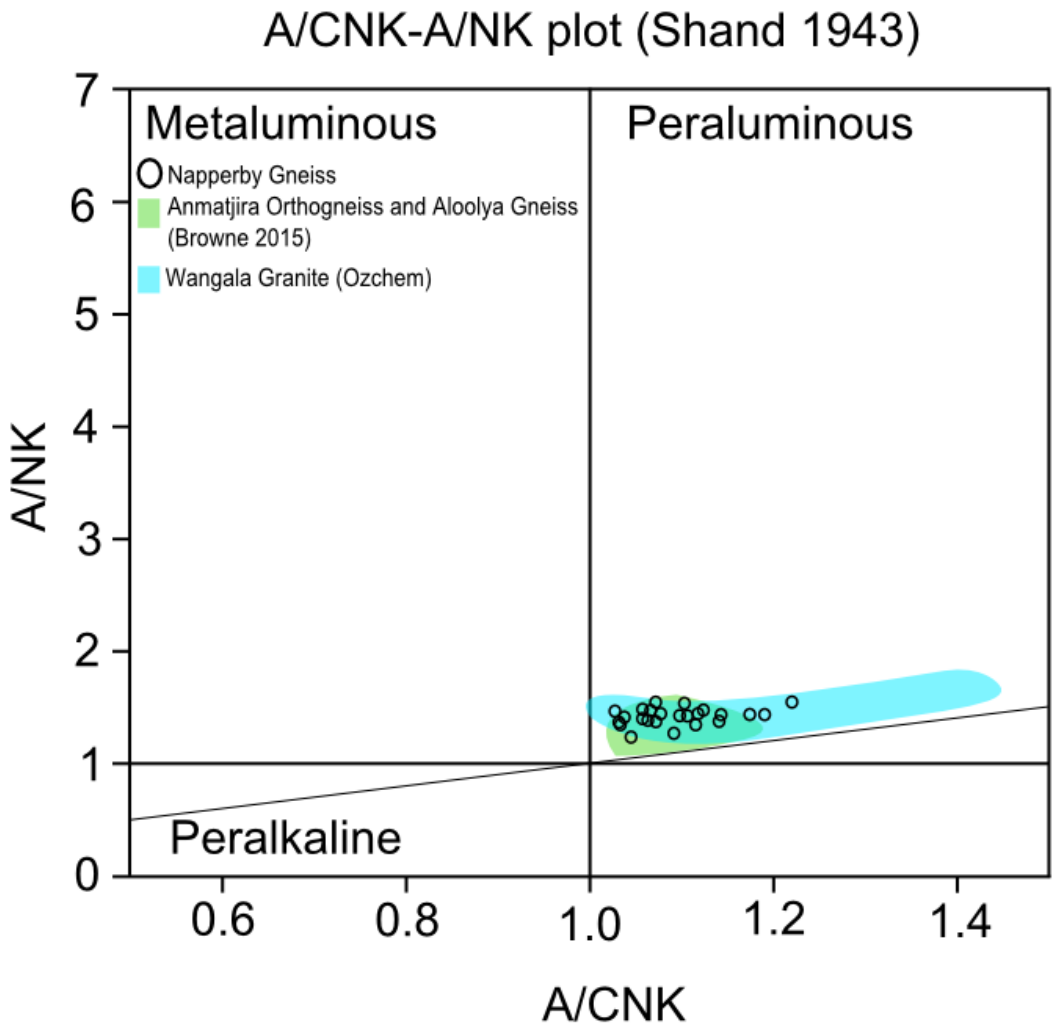

Figure 7: Alumina Saturation Index following Shand (1943), showing Napperby data and granites from the Anmatjira Range (Browne 2015) and the Wangala Granite (Ozchem).

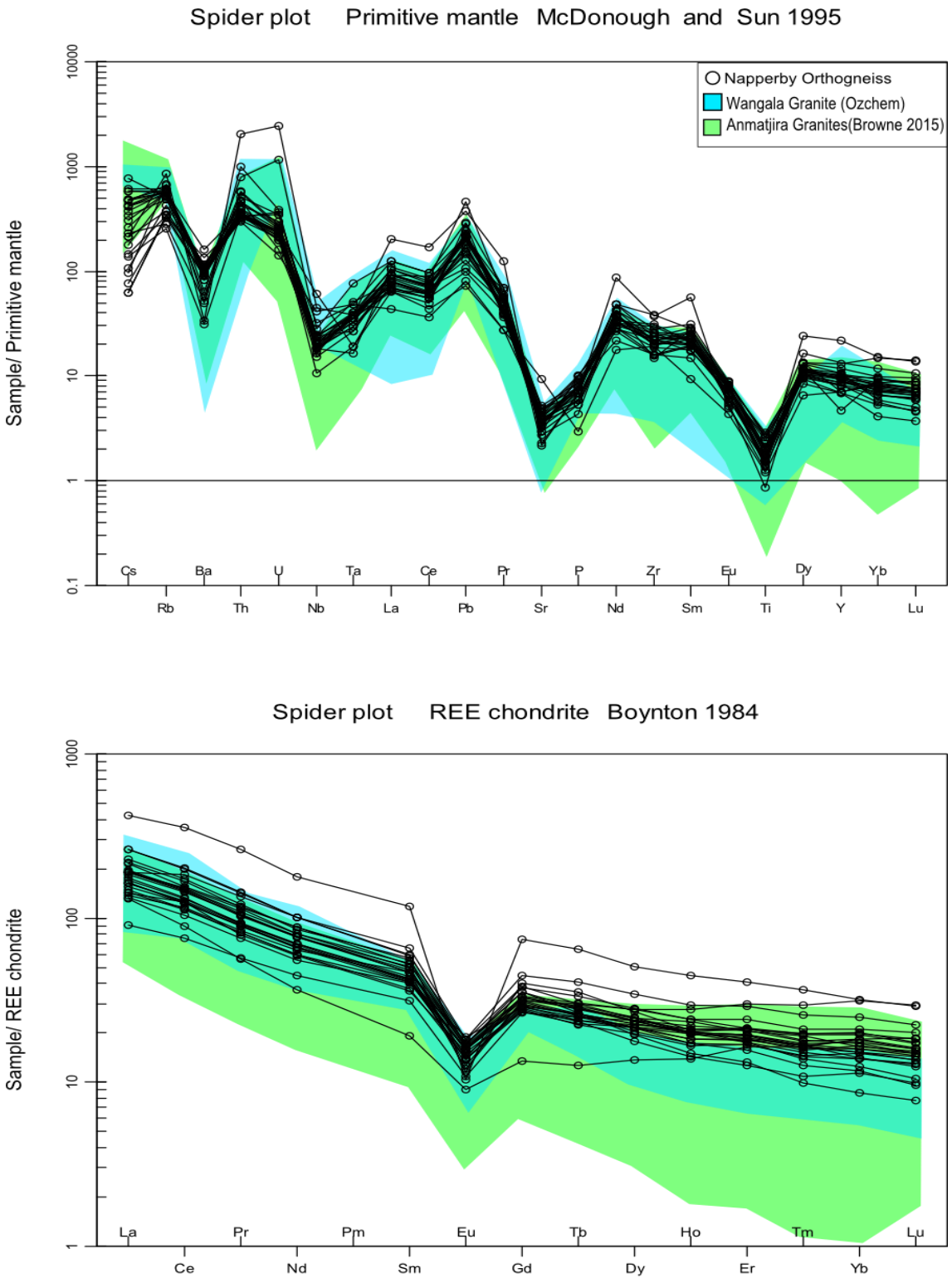

Figure 8: Spiderplots of trace and rare earth elements normalised to (a) Primitive Mantle (McDonough and Sun 1995) and (b) Chondrite (Boynton 1984) respectively.

4.2.3 RADIOGENIC ISOTOPES

Seven samples of the Napperby Gneiss along with one sample of the metasedimentary raft were selected for Sm–Nd isotope analysis. Table 2 shows the data collected including εNd values and depleted mantle model ages. The εNd vs. time plot illustrated in Figure 9 shows the eight data points along with other Nd datasets from the Arunta Region (Brown 2015, Lau pers. comm. 2016, NTGS STRIKE).

The depleted mantle and CHUR evolution lines are indicated as well as the evolution of regional Archaean crust, based on the ca 2500Ma Tanami region Billabong complex (NTGS STRIKE), and the evolution of the Stafford Beds, representative of the Lander Formation. The εNd values of the Napperby Gneiss range from -1.6 to -8.8, and the values of the metasedimentary raft is -6.1.

Table 2: Radiogenic Isotopic data from Sm–Nd analyses, used to plot εNd-T diagram

Sample	*Rock Unit*	*Sm(ppm)*	*Nd(ppm)*	*147Sm/144Nd*	*143/144Nd(0)*	*2σ(x1E-6)*	*εNd (1780)*	*T_{DM}(Ma)*
72921017	Napperby Gneiss	11.7	60.3	0.1310	0.511588	2.17	-5.5	2833
85924153	Napperby Gneiss	23	107.5	0.1448	0.511582	2.11	-8.8	3403
85924167	Napperby Gneiss	10.1	52.6	0.1200	0.511468	2.32	-5.3	2697
85924196	Napperby Gneiss	3.75	22	0.1039	0.511469	1.46	-1.6	2307
NAP2010-5	Napperby Gneiss	11.2	51.3	0.1378	0.511679	1.54	-5.3	2907
NAP2010-6	Napperby Gneiss	9.66	48.1	0.1205	0.511519	1.56	-4.5	2630
NAP2010-7	Napperby Gneiss	10.85	53	0.1249	0.511615	2.09	-3.6	2599
NAP2012-11A	Metasedimentary raft	9.6	58.3	0.1050	0.511253	1.78	-6.1	2626

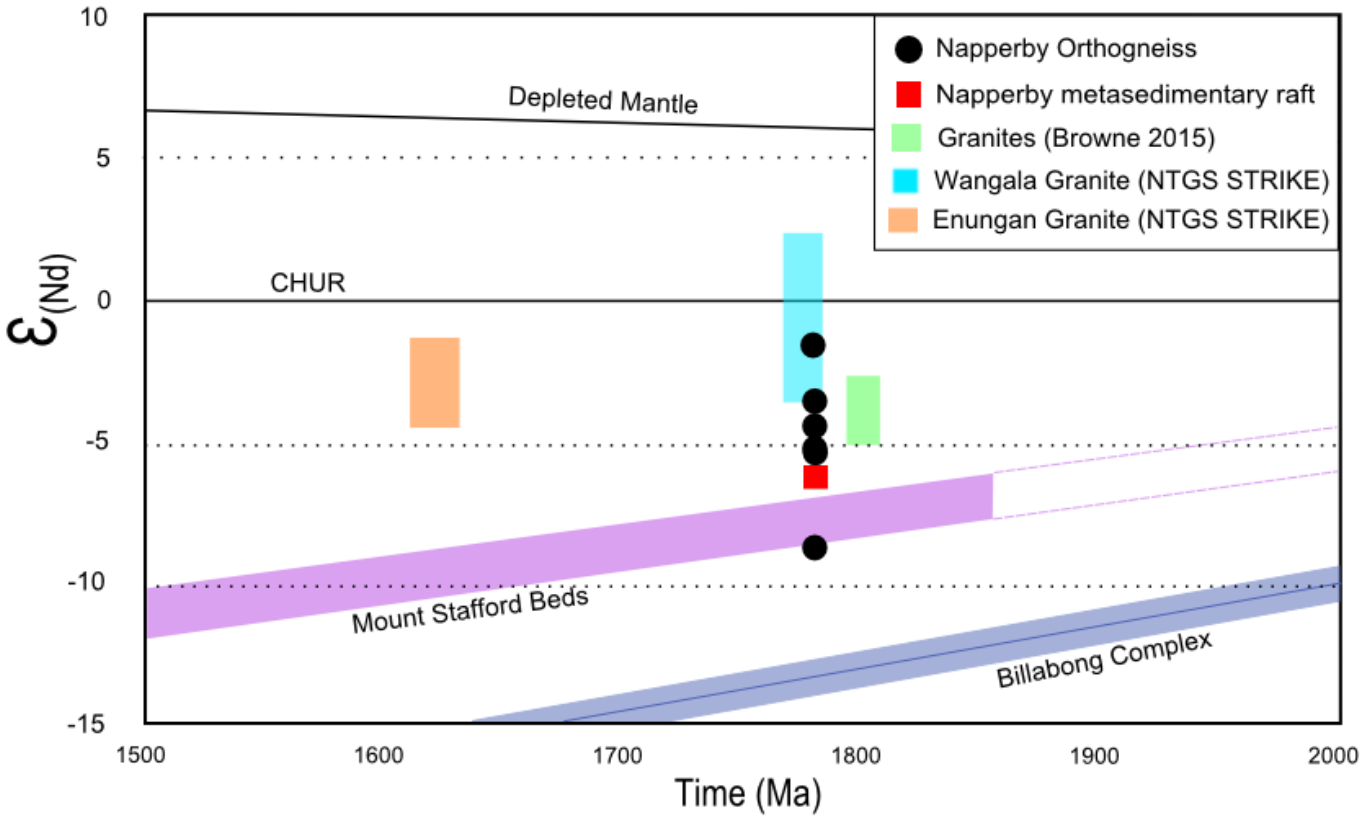

Figure 9: Epsilon-Neodymium vs time diagram illustrating samples from this work along with data from Browne and the NTGS database. Archaean crustal evolution is represented by the Billabong Complex, with The Mount Stafford Beds representing local basement.

4.2.4 RADIOGENIC HEAT PRODUCTION

Table 3 shows average calculated heat production values using K%, U (ppm) and Th (ppm) at crystallisation age.

The average heat production for the Napperby Gneiss with an age of 1780 Ma was 5.21 μWm^{-3} but ranges up to 11.03 μWm^{-3} (Figure 10).

Global averages of crustal heat production were taken from Wedepohl (1995), with a corresponding silica values from Gao & Rudnock (2014). Lander Formation values were calculated from data retrieved from OZCHEM, and a Post Archean average Australian Shale value of 2.15 μWm^{-3} (PAAS; Taylor and McLennan 1985).

Figure 11 shows the εNd values plotted against heat production. More negative εNd values have higher heat production.

Table 3: Heat production calculations from whole rock geochemistry data

Sample	*Rock Unit*		*K wt%*	*Th ppm*	*U ppm*	*ΔTime (Ma)*	*Heat* **Production (μWm^{-3})**
Global AVG UPPER continental crust		*Wedepohl 1995*	2.865	10.3	2.5	0	1.69
Global Avg Lower continental crust		*Wedepohl 1995*	1.314	6.6	0.93	0	0.85
Whole crust avg		*Wedepohl 1995*	2.14	8.5	1.7	0	1.27
72921017	Napperby Gneiss		4.018	63.4	23	1780	11.03
72921019	Napperby Gneiss		3.362	30.5	4.57	1780	3.74
85924153	Napperby Gneiss		5.512	165.5	48.9	1780	25.38
85924155	Napperby Gneiss		4.001	44.9	5.25	1780	5.03
85924167	Napperby Gneiss		3.844	31.6	4.94	1780	3.97
85924196	Napperby Gneiss		2.623	36.8	5.35	1780	4.33
85924200	Napperby Gneiss		3.819	26	4.68	1780	3.49
85924162C	Napperby Gneiss		4.292	33.8	5.94	1780	4.44
85924163A	Napperby Gneiss		3.985	46.7	5.47	1780	5.22
85924183A	Napperby Gneiss		3.943	27.3	7.02	1780	4.21
NAP2010-11	Napperby Gneiss		4.018	24.8	4.19	1780	3.30
NAP2010-12	Napperby Gneiss		3.786	27.4	4.29	1780	3.49
NAP2010-2	Napperby Gneiss		2.225	27.5	4.34	1780	3.35
NAP2010-3	Napperby Gneiss		3.337	27.4	4	1780	3.37
NAP2010-4	Napperby Gneiss		3.263	28	4.63	1780	3.57
NAP2010-5	Napperby Gneiss		5.587	79.5	7.76	1780	8.36
NAP2010-6	Napperby Gneiss		4.499	37.5	3.21	1780	4.01
NAP2010-7	Napperby Gneiss		4.026	36.5	5.07	1780	4.38
NAP2010-8	Napperby Gneiss		4.881	28.1	4.92	1780	3.81
NAP2010-9	Napperby Gneiss		4.790	26.4	7.4	1780	4.33
NAP2012-10	Napperby Gneiss		3.761	29.3	3.95	1780	3.53
NAP2012-11a	Metasedimentary Raft		3.022	26.8	3.85	0	3.25
NAP2012-12	Napperby Gneiss		4.342	40.8	6.95	1780	5.21
NAP2012-15	Napperby Gneiss		3.777	28.9	4.86	1780	3.75
NAP2012-4	Napperby Gneiss		4.226	29.4	4.64	1780	3.77
NAP2012-6	Napperby Gneiss		4.134	27.4	4.63	1780	3.61
NAP2012-8	Napperby Gneiss		3.561	23.7	2.86	1780	2.82

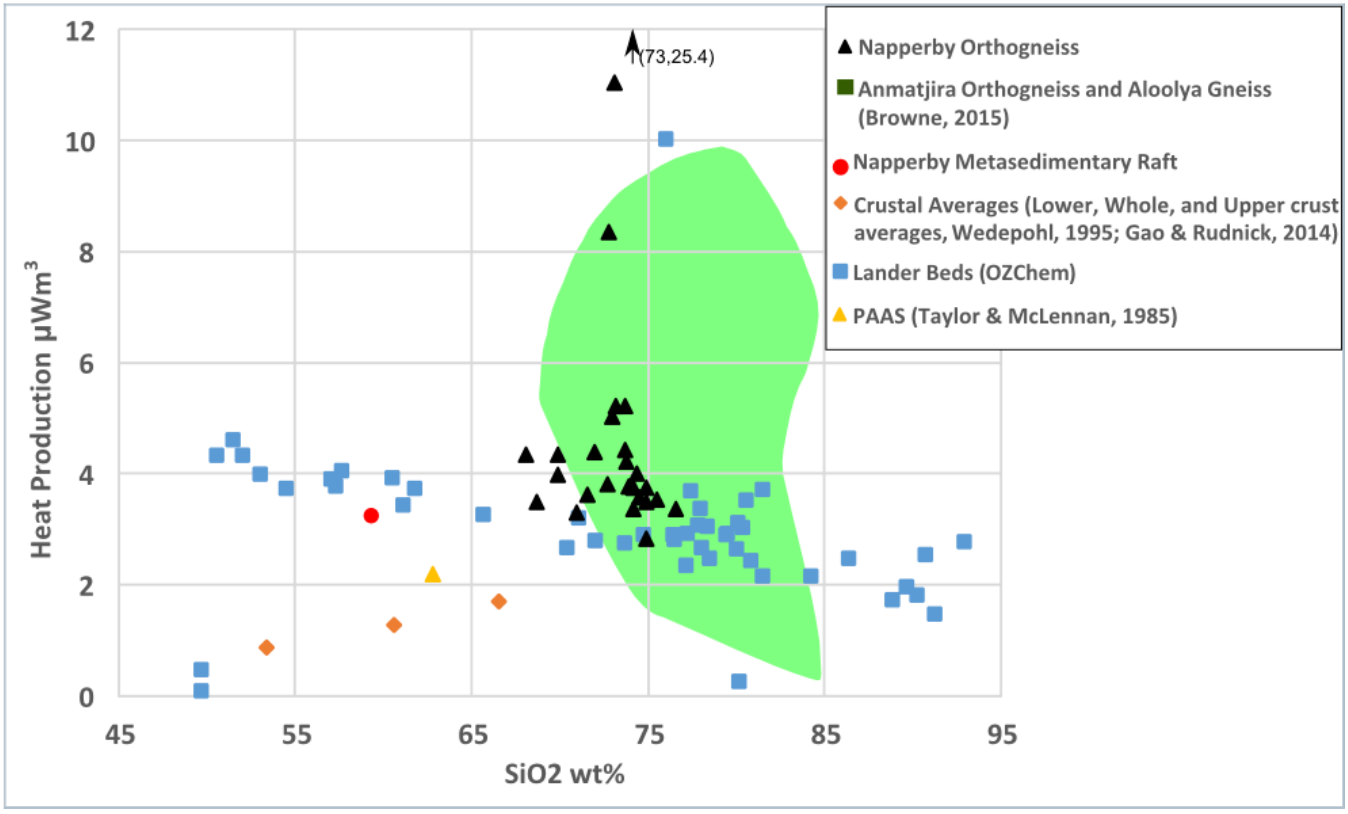

Figure 10: Heat production values calculated for the Napperby Gneiss (5.21) and the surrounding Lander Formation, and granitic rocks from the Anmatjira Range (5.58 and 2.97); along with PAAS and global crustal averages.

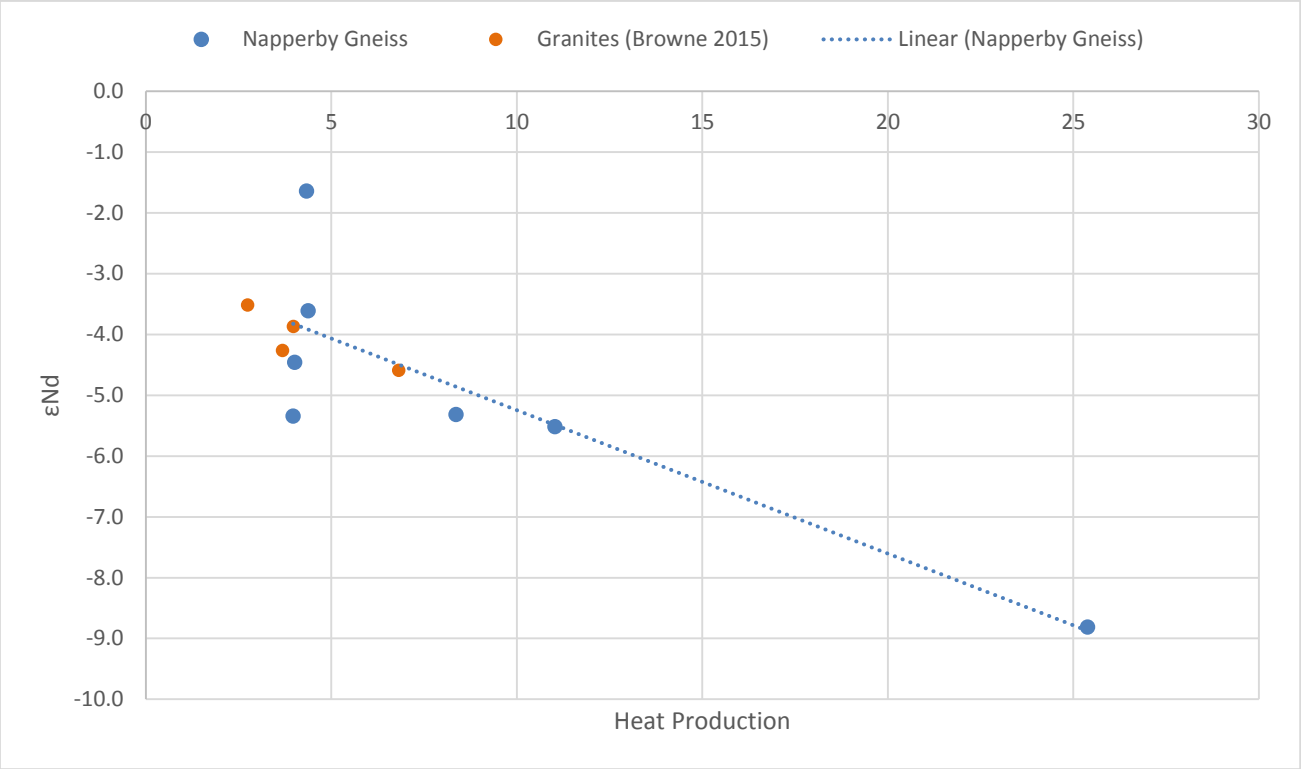

Figure 11: showing εNd values against corresponding heat production values, and comparing the Napperby to the Aloolya Granite and Anmatjira Orthogneiss (Browne 2015).

4.3 Geochronology

U-Pb dating of zircons was undertaken to examine the nature of the crust that contributed to the source of the Napperby Gneiss. Previous work has indicated the orthogneiss precursor granite is moderately peraluminous (Collins and Williams 1995) suggesting crustal sedimentary material contributed to its source region. The base of the oldest units in the region, the widespread Lander formation is not identified. As most peraluminous granites contain substantial inherited zircon the age pattern of xenocrystic zircons in the orthogneiss was compared to the detrital zircon pattern of surrounding metasedimentary rock and the metasedimentary raft to enable interpretations of potential source rocks at depth.

4.3.1 INHERITED ZIRCON AGES

Figure 12 shows the population patterns of zircons from the Napperby Gneiss, Metasedimentary Raft, Reynolds range Group, and Lander Formation.

Comparison of Napperby Gneiss (11C) and the Metasedimentary Raft (11A) shows the dominant inherited age peak (ca. 1830 Ma) from the orthogneiss aligns with that of the detrital zircons of the metasedimentary raft. There are differences in older peaks between the two which could be due to differences in sample size or overprinting by metamorphic events within the Reynolds Ranges.

Comparison of the Napperby Gneiss (11C) compared to the detrital zircon signature of the Mount Thomas Quartzite (11B), which is the basal unit of the Reynolds Range Group (Claoue-Long et al. 2008; Rosel et al. 2014), shows similar patterns. However the Napperby lacks the age peak of sub-1800 Ma zircons seen in the Reynolds Range Group.

Comparison of zircon population signatures of the Napperby Gneiss (11C) and the Lander Formation (11D), compiled from Claoue-Long et al. (2008), and Vry et al. (1996), show broad similarities. The dominant inherited peak is younger than that of the youngest detrital population in the Lander Formation. However the older peaks from the Napperby Gneiss are a closer match to those of the Lander Formation than the Reynolds Range Group. Discrepancies between the patterns may be due to differences in sample size or possible overprinting by metamorphic events.

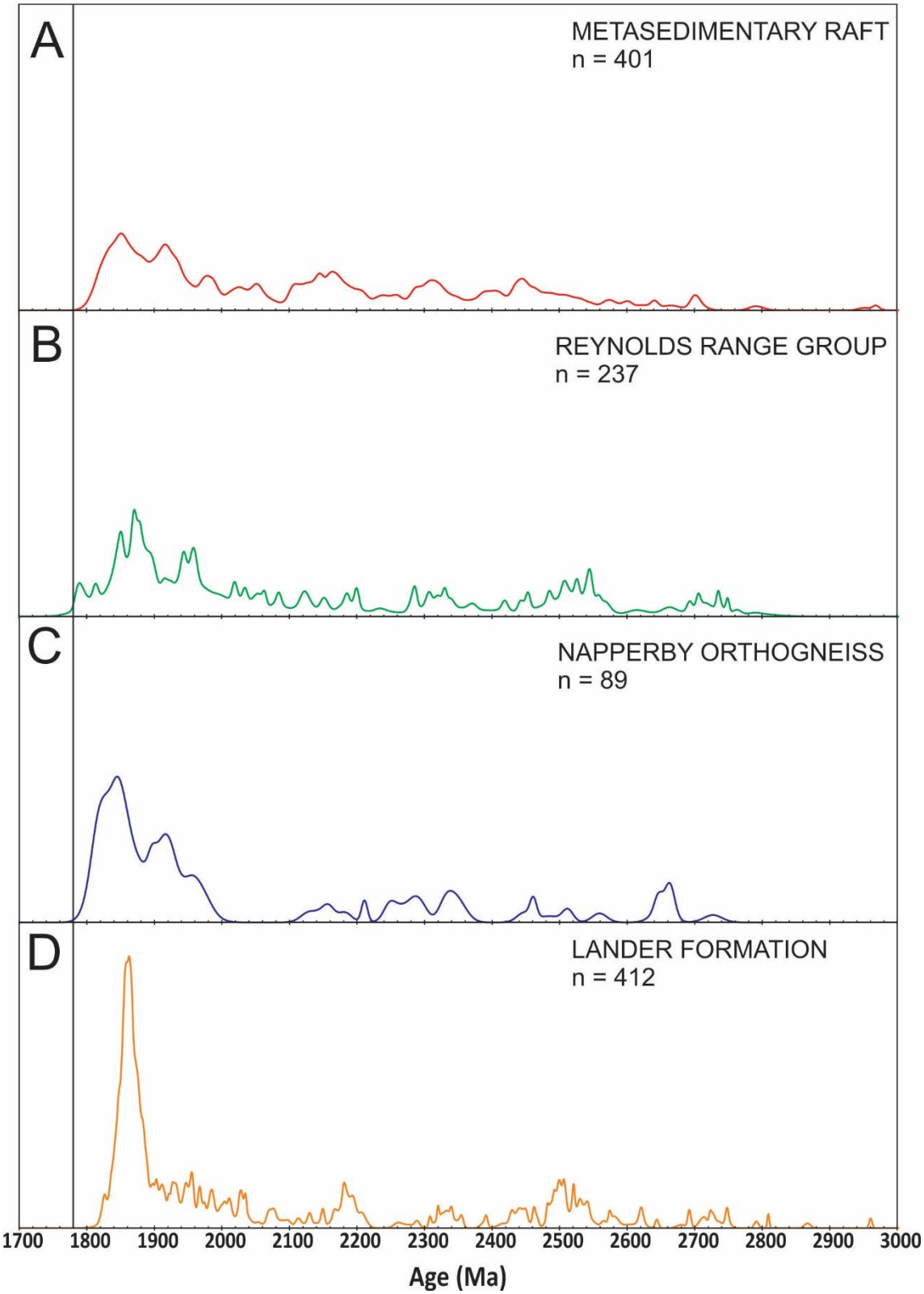

Figure 12: Probability Density plots of 207Pb/206Pb ages showing complied data for: (A) The Metasedimentary Raft from this study and literature (Reid 2012); (B) The Reynolds Range Group from literature (Claoue-Long et al. 2008; Rosel et al. 2014); (C) compiled data for the Napperby Gneiss from this study and literature (Collins and Williams 1995, Reid 2012); (D) The Lander Formation from literature (Claoue-Long et al, 2008, Vry et al, 1996). The black line represents the intrusive age for the precursor to the Napperby Gneiss.

4.4 Zircon Saturation Thermometry

Zircon saturation thermometry was carried out following the work of Watson and Harrison (1983) modified by Boehnke et al. (2013). The Napperby Gneiss yielded temperatures ranging from 790 ˚C to 872 ˚C, with an average temperature of 827 ˚C, in comparison the granites of the Anmatjira range, which have colder temperatures ranging from 585°C to 805 °C, and an average of 746°C. The Wangala granite yields temperatures which range from 708°C to 842°C, with an average of 788°C.

Table 4: Zircon Saturation Thermometry Calculations from whole rock geochemistry data

Sample ID	Zr ppm	Total Heat Production	M value	Temp (˚C)
72921017	246	11.03	1.37	827.04
72921019	232	3.74	1.35	823.52
85924153	388	25.38	1.38	870.86
85924155	265	5.03	1.35	836.15
85924167	275	3.97	1.37	838.26
85924196	199	4.33	1.43	803.16
85924200	194	3.49	1.26	813.71
85924162C	227	4.44	1.32	823.55
85924163A	399	5.22	1.41	871.44
85924183A	312	4.21	1.36	850.88
NAP2010-11	264	3.30	1.40	831.88
NAP2010-12	232	3.49	1.34	824.61
NAP2010-2	229	3.35	1.29	826.88
NAP2010-3	218	3.37	1.26	824.47
NAP2010-4	210	3.57	1.29	818.89
NAP2010-5	155	8.36	1.31	790.09
NAP2010-6	213	4.01	1.23	824.70
NAP2010-7	226	4.38	1.28	826.65
NAP2010-8	168	3.81	1.19	806.23
NAP2010-9	165	4.33	1.25	800.12
NAP2012-10	246	3.53	1.37	827.21
NAP2012-12	293	5.21	1.24	854.69
NAP2012-15	227	3.75	1.25	829.74
NAP2012-4	207	3.77	1.27	819.36
NAP2012-6	328	3.61	1.22	867.72
NAP2012-8	169	2.82	1.34	795.17

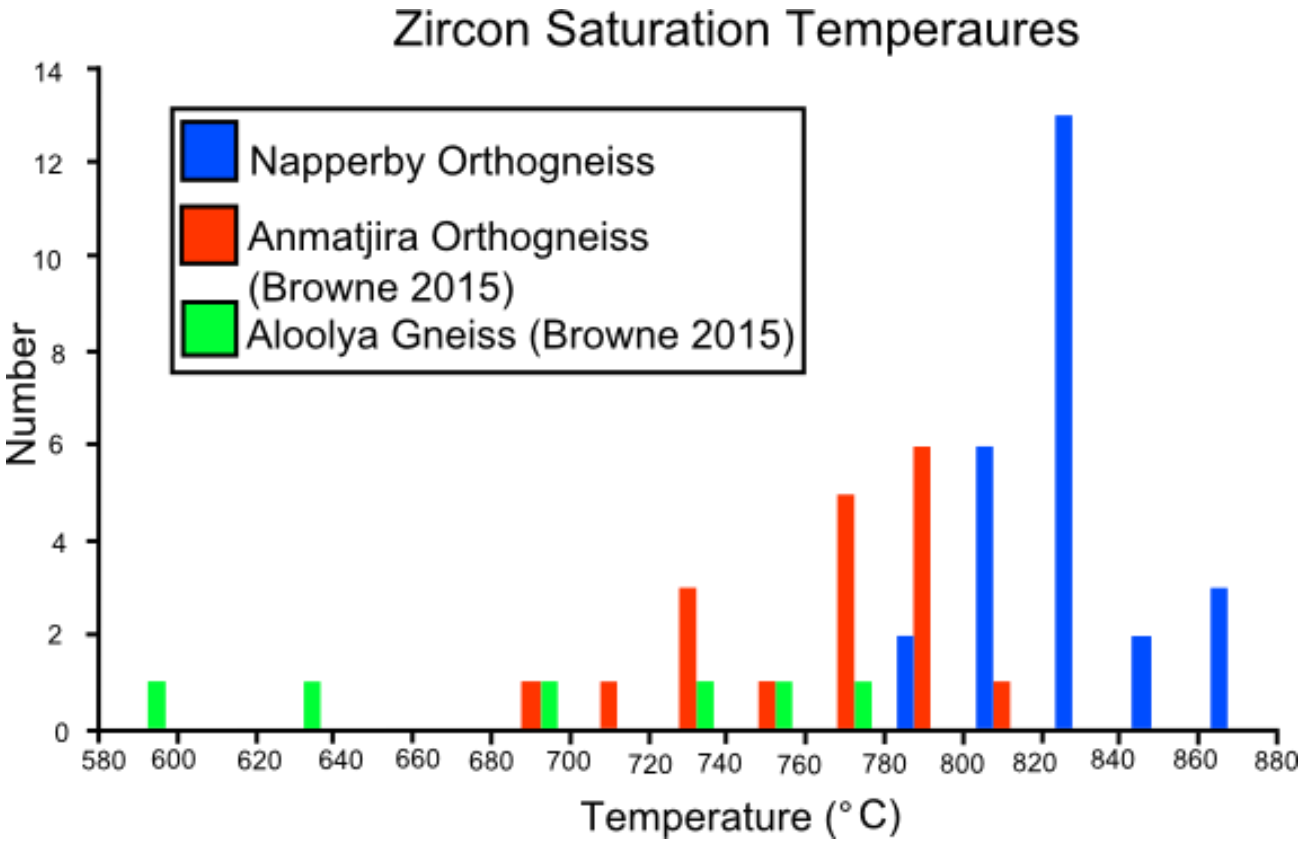

Figure 13: Histogram of Zircon Saturation temperatures, comparing those of the Napperby to those of the granites of the Anmatjira range (Browne 2015).

5 DISCUSSION

5.1 Geochemical characterisation of the Napperby Gneiss

Chappell and White (1974) proposed that the geochemistry of granitoids reflects the geochemistry of their source rock. Peraluminous granites are most likely the result of melting of a metasedimentary material (Garcia et al, 1994). As the Napperby Gneiss plots as peraluminous (Figure 7) in the Shand (1943) classification scheme, this suggests that it was produced by the melting of a sedimentary package.

The Napperby Gneiss does not exhibit strong fractionation trends in major elements (Figure 6), especially when compared to the ca. 1800 Ma (Browne 2016) granites of the Anmatjira range and the 1775 Ma Wangala granite of Mount Denison (Beyer 2012, Scrimgeour 2013). The Napperby Gneiss and the Wangala granite show similar geochemical trends, with strong similarities seen in Al2O3, MgO, K2O, P2O5, and Fe2O3 harker plots, along with very similar trace element and REE trends (Figure 9). This geochemical similarity along with close spatial and temporal relationships suggests that the Wangala granite and the Napperby Gneiss are co-magmatic.

There are slight variations in the REE patterns of the Napperby Gneiss which can be contributed to the heterogeneity of the crust or possibly variations in the fraction of crustal or mantle melt components of each sample. Negative Eu anomalies in granitic samples suggest that they plagioclase in the residue (Weill & Drake, 1973). Further evidence for residual plagioclase is slight depletion in Ba, and depletion of Sr, compared with other adjacent elements (Figure 8). Al_2O_3 and CaO both decrease with increasing SiO_2, which further supports fractionation of plagioclase.

The geochemical trends exhibited by the Napperby Gneiss are consistent with those of the ca 1780-1750 Ma ‘Low-Al type Main Group’ of Arunta granites, as put forth by

Zhao & McCulloch (1995), and believed to show influence of arc-type geochemical signatures.

As seen in the εNd diagram (Figure 9) the samples of the Napperby Gneiss analysed show a range of slightly to more negative εNd values. One value lies within the range of Lander Formation and equivalent units while the others form a spread from the value of the metasedimentary raft to less negative values. This variation in εNd values suggests that the parent magma would have been a mix of both the pre-existing crust and also some juvenile mantle derived magma.

It has been proposed by McLaren and Powell (2014), that granites of the Proterozoic Australia first underwent the addition of a juvenile mafic source into the lower crust. This was followed by melting of the lower and upper crust with the heat from the mafic source assisting in this melting. This could account for the mafic influence which in observed in granite suites across the Arunta (Figure 9).

The εNd values of the samples in this study suggest an evolved crustal source of the granites. This, combined with the knowledge that the granites are peraluminous, implies the major source component was a metasedimentary unit.

5.2 A Possible Source

Previous work on the sedimentary packages of the Reynolds Ranges has shown that the detrital zircon pattern of Lander Rock Formation forms a dominant peak between 1880 – 1830 Ma with a subordinate presence of older grains up to ca. 2750 Ma, while those of the Reynolds Range Group are spread across a range of 2700 to 1870 Ma with a population at 1820-1785 Ma (Claoue-Long et al., 2008a). U-Pb ages from previous studies of this Formation (Claoue-Long et al., 2008, Vry et al., 1996) and the Reynolds Range Group (Claoue-Long et al., 2008a; Rosel et al. 2015), were compared to ages for

the Napperby Gneiss from this and previous studies (Collins & Williams, 1995; Reid 2012) and the metasedimentary raft within the Napperby (Reid 2012).

Figures 12a and 12c show the detrital pattern of the Metasedimentary Raft and the Napperby Gneiss. These patterns are extremely similar, with the orthogneiss and the metasediment sharing most population peaks with slight difference in older populations. These differences are likely due to differences in size of the sample populations.

Figures 12b and 12d show the detrital zircon population patterns of the Reynolds range Group and the Lander Formation respectively, compared with the inherited zircons of the Napperby Gneiss (Figure 12c). The Napperby Gneiss' xenocrystic zircons shown a population pattern which lacks the younger 1800-1780 Ma population which is distinctive of the Reynolds Range Group, its populations of older zircons more closely match those of the Lander Formation compared to the Reynolds Range Group. The dominant peak of the Napperby Gneiss is slightly younger than that of the Lander Formation, possibly due to differences in sample size or metamorphic overprinting of zircons.

In the field the Napperby Gneiss intrudes the Reynolds Range Group (Scrimgeour, 2013), and the Reynolds Range Group unconformably overlies the Lander Formation (Claoue-Long et al. 2008; Scrimgeour, 2013). This relationship means that the Reynolds Range group could not be the source rock. The Lander Formation or an older sedimentary package with similar geochronological characteristics are the most likely crustal source for the Napperby's granitic precursor.

5.3 Sources of enrichment in Heat Producing Elements

Whole Rock Geochemistry from OZCHEM of the Lander Rock Formation shows that it is enriched in U, Th and K when compared to post-Archean Australian Shale (Taylor

and McClennan, 1985) and average levels of the continental crust (Wedepohl, 1995). The metasedimentary raft has a heat production of 3.25 μWm^{-3}, within the greater trend of the Lander Formation. The Napperby Gneiss has an average heat production of 4.40 μWm^{-3} only just above that of the Lander Formation (3.11 μWm^{-3}). Bea (2012) stated that a metasedimentary rock that is enriched in heat producing elements (HPE) will produce a granite that is enriched in HPE. As such the elevated heat production of the Lander Formation, compared to global averages, supports a Lander equivalent being the source of the crustal component of the Napperby Gneiss.

The granitoides of the Anmatjira range have an average heat production of 5.68 μWm^{-3} and 2.97 μWm^{-3} for the Anmatjira orthogneiss and Alooyla granite respectively (Browne 2015). The Anmatjira orthogneiss shows a significantly higher average heat production value compared to the Napperby Gneiss over similar silica range. The Aloolya gneiss exhibits low heat production values compared to the Napperby Gneiss, this is likely due to the Aloolya granite being both highly fractionated and highly weathered (Browne 2016).

5.4 Zircon Saturation Thermometry and Tectonic Implications

Zircon saturation temperatures are an important tool in the estimation of magma temperatures at the source. The Napperby Gneiss is a relatively 'hot' granite with an average zircon saturation temperature of 827 ˚C, the generation of which requires a large heat influx rather than a large fluid influx need by 'cold' granites (Miller et al. 2014). Miller et al continues further saying that a majority of hot granites are emplaced extensional or trantensional terranes, and often have erupted equivalents.

The Napperby Gneiss is a 'hot' granite compared with the 'colder', ca. 1800 Ma granites of the Anmatjira range (Figure 12). The zircon saturation thermometry suggests a change in melting styles within the 20 Ma period from the 'cold', fluid influx melting of the Anmatjira range granites to the 'hot', heat influx style of the Napperby's granitic precursor. The differences in the proposed melting styles would have influence in the budget of U, Th and LREE elements in the different granitic melts, as both have Lander Formation equivalent metasedimentary sources. Monazite is a significant control on the LREE availability in granitic liquids, and monazite dissolution is largely controlled by the presence of fluids in the melt (Watt and Harley 1993, Aranovich et al 2014). The increased presence of fluids in the melt that produced the Anmatjira granites would have led to increased dissolution of monazite into the melt, which can be seen in the increased heat production of the Anmatjira orthogneiss compared to the Napperby Gneiss.

The prevalent view on the tectonic environment of the Arunta region Paleoproterozoic is that of a long lived active margin, a series of related island-arc/back-arcs systems, along the current day southern margin of the North Australian Craton (Scrimgeour et al. 2005, Betts & Giles 2006, Cawood & Korch 2008; Zhao and McCulloch 1995; Sun et al. 1995; Zhao 1994). The Napperby Gneiss is part of the Low-Al Main Group as proposed by Zhao and McCulloch (1995), believed to have formed by partial melting of arc-type underplates or intrusions during collision of island arcs. However they go on to concluded that the geochemical signatures of the 'Main Group' of granites have arc-influenced but ambiguous trace element characteristics in relation to tectonic discrimination.

The zircon saturation thermometry, along with ambiguous geochemical signature of Zhao and McCulloch's Main Group, suggests that the precursor to the Napperby Gneiss formed an extensional tectonic setting, possibly a back-arc related to the long-lived subduction that derived the older granites of the Anmatjira Range.

6 CONCLUSIONS

The Paleoproterozoic Napperby Gneiss, aged 1780 Ma, is enriched in U and Th, resulting in a high heat producing granite. The εNd values of the Napperby Gneiss range from -1.1 to -8.2, suggesting that it was derived from an evolved crustal source with some juvenile component. Additionally, geochemical analysis shows that the Napperby Gneiss is moderately peraluminous and as such can be said to have a metasedimentary source. The Napperby Gneiss contains a metasedimentary raft, which has a near identical zircon probability density pattern, which when combined with εNd data suggest it is an enclave of the metasedimentary source rock. The detrital zircon ages of the metasedimentary raft and the inherited ages of the Napperby compare well with those of the Lander Formation. Zircon saturation thermometry shows that the Napperby Gneiss is a hot granite and suggests that it is a dry granite formed by heat flux in an extensional setting. The presented evidence suggests that the most likely source for the high heat producing Napperby Gniess is a unit equivalent or older to the Lander Formation with contribution of juvenile material.

ACKNOWLEDGMENTS

I would like to thank Karin Barovich for the support and guidance throughout the year, and always being available for advice. I would like to extend my thanks to Martin Hand and WingKei Lau for their assistance and input. Thanks to David Bruce for help with collecting and analysing isotopic data, and assistance in the lab. Aoife McFadden, Ben Wade and the rest of the staff and Adelaide Microscopy are thanked for their help and guidance with SEM imaging and LA-ICP-MS analysis. Thanks to Katie Howard for all her help throughout the year, and her patience in doing so. Finally my thanks and gratitude to the 2016 Honours Group for making this such a great year

REFERENCES

ARANOVICH L. Y., MAKHLUF A. R., MANNING C. E. & NEWTON R. C. 2014 Dehydration melting and the relatinship between granites and granulites, *Precambrian Research,* **253**, 26-37.
BEA F. 2012 The sources of energy for crustal melting and the geochemistry of heat-producing elements, *LITHOS,* **153**, 278-291.
BETTS P. G. & GILES D. 2006 The 1800–1100 Ma tectonic evolution of Australia, *Precambrian Research,* **144**, 92-125.
BEYER E. E., ALLEN C. M., ARMSTRONG R. & WOODHEAD J. D. 2015 Summary of results; NTGS laser ablation ICPMS U-Pb and Hf geochronology project; selected samples from Napperby 1:250 000 mapsheet area, Arunta region, July 2010-January 2012. Northern Territory Geological Survey.
BOEKNKE P., WATSON E. B., TRAIL D., HARRISON T. M. & SCHMITT A. K. 2013 Zircon saturation re-revisited, *Chemical Geology,* **351**, 324-334.
BROWNE J. 2015 Geochemical and isotopic investigation into the source of U and Th enrichemnt in the Prtoerozoic, high heat producing granites of the Anmatjira Range. Honours thesis. University of Adelaide, Adelaide (unpubl.).
BOYNTON W. V. 1984. Geochemistry of the rare earth elements: Meteorite studies. In: Henderson P. ed. Rare earth element geochemistry, 63–114. Elsevier.
BUDD A. R., HAZEL M. S., SEDGMEN A., SEDGMEN L., WYBORN L. & RYBURN R. 2000 OZCHEM dataset release 1 documentation: AGSO's natinal whole rock geochemistry database. Record 2000/012, *Australian Geological Survey Organisation, Canberra*.
BUICK I. S., MILLER J. A., I.S. W. & CARTWIRGHT I. 2001 Ordovician ghigh-grade metamorphism of a newly recognised late Neoproterozoic terrane in the northern Harts Range, central Australia, *Journal of Metamorphic Geology,* **19**, 373 - 394.
CARTWIRGHT I., BUICK I. S., FOSTER D. A. & D. L. D. 1999 Alice Springs age shear zones from teh southeastern Reynolds Range, central Australia, *Australian Journal of Earth Sciences,* **46**, 355-363.
CAWOOD P. A. & KORSCH R. J. 2008 Assembling Australia: Proterozoic building of a continent, *Precambrian Research,* **166**, 1-35.
CHAPPELL B. W. & WHITE A. J. R. 1974 Two contrasting granite types, *Pacific Geology,* **8**, 173-174.
CLAOUÉ-LONG J., EDGOOSE C. & WORDEN K. 2008 A correlation of Aileron Province stratigraphy in central Australia, *Precambrian Research,* **166**, 230-245.
CHEW, D.M., PETRUS, J.A. & KAMBER, B.S. 2014 U-Pb La-ICPMS dating using accessory mineral stadndars with variable common Pb, Chemical Geology, 365, 185-199
COLLINS W. J. & VERNON R. H. 1991 Orogeny associate with anticlockwise P-T-t paths; evidence from low-P. high-T metamorphic terranes in the Arunta Inlier, central Australia, *Geology,* **19**, 835-838.
COLLINS W. J. & SHAW R. D. 1995 Geochronological constraints on orogenic events in the Arunta Inlier - a review, *Precambrian Research,* **71**, 315-346.
COLLINS W. J. & WILLIAMS I. S. 1995 SHRIMP ionprobe dating of short-lived Proterozoic tectonic cycles in the northern Arunta Inlier, central Australia, *Precambrian Research,* **71**, 69-89.
DIRKS P. & WILSON C. J. L. 1990 The geological evolution of the Reynolds Range, central Australia: evidence for three distinct structural-metamorphic cycles, *journal of Structural Geology,* **12**, 651-665.
DIRKS P. & HAND M. 1991 Structural and metamorphic controls on the distribution of zircon in an evolving quartzofeldspathic migmatite; an example from the Reynolds Range, central Australia, *Journal of Metamorphic Geology,* **9**, 191-201.
DIRKS P., HAND M. & POWELL R. 1991 the P-T-deformation path for a mid-Proterozoic, low pressure terrane; the Reynolds Range, central Australia, *Journal of Metamorphic Geology,* **9**, 641-661.
DIRKS P. H. G. M. 1990 Intertidal and subtidal sedimentation during a mid-Proterozoic marine transgression, reynolds range group, Arunta block, central Australia, *Australian Journal of Earth Sciences,* **37**, 409-422.
GARCIA D., FONTEILLES M. & MOUTTE J. 1994 Sedimentary Fractionations between Al, Ti, and Zr and the Genesis of Strongly Peraluminous Granites, *The Journal of Geology,* **102**, 411-422.
GILES D., BETTS P. & LISTER G. 2002 Far-field continental backarc setting for the 1.80-1.67 Ga basins of northeastern Australia, *Geology (Boulder),* **30**, 823-826.
HAND M. & BUICK I. S. 2001 Tectonic evolution of the Reynolds-Anmatjira Ranges: A case study in terrain reworking from the Arunta Inlier, central Australia, *Geological Society Special Publication,* **184**, 237-260.
HAWKESWORTH C. J., DHUIME B., PIETRANIK A. B., CAWOOD P. A., KEMP A. & STOREY C. D. 2010 The generation and evolution of the continental crust. J. Geol. Soc., **167**, 229-248.

HOATSON D. M., SUN S. & CLAOUE-LONG J. C. 2005 Proterozoic mafic-ultramafic intrusions in the Arunta Region, central Australia Part 1: Geological setting and mineral potential, *Precambrian Research*, **142**, 93-133.
KEMP A. I. S., HAWKESWORTH C. J., FOSTER G. L., PATERSON B. A., WOODHEAD J. D., HERGT J. M., GRAY C. M. & WHITEHOUSE M. J. 2007 Magmatic and crustal differentiation history of granitic rocks from Hf-O isotopes in zircon, *Science (New York, N.Y.)*, **315**, 980.
MCDONOUGH W. F. & SUN S.-S. 1995. The composition of the Earth. Chemical Geology 120, 223-253
MCLAREN S., SANDIFORD M., HAND M., NEUMANN N., WYBORN L. & BASTRAKOVA I. 2003 The hot southern continent: heat flow and heat production in Australian Proterozoic terranes, *Geological Soiciety of Australia Special Publication*, **22**, 151 -161.
MCLAREN S., SANDIFORD M. & POWELL R. 2005 Contrasting styles of Proterozoic crustal evolution a hot-plate tectonic model for Australian terranes, *Geology (Boulder)*, **33**, 673-676.
MCLAREN S. & POWELL R. 2014 Magmatism, orogeny and the origin of high-heat-producing granites in Australian Proterozoic terranes, *Journal of the Geological Society of London*, **171**, 149-152.
MIDDLEMOST E. A. K. 1994 Naming materials in the magma/igneous rock system, *Earth-Science Reviews*, **37**, 215-224.
MILLER C. F., MCDOWELL S. M. & MAPES R. W. 2003 Hot and cold granites? Implications of zircon saturation temperatures and preservation of inheritance, *Geology*, **31**, 529-532.
PAYNE J. L. B., KARIN M.; HAND, MARTIN 2006 Provenance of metasedimentary rocks in the northern Gawler Craton, Australia: Implications for Palaeoproterozoic reconstructions, *Precambrian Research*, **148**, 275-291.
R. S., STEWART A. & BLACK L. 1984 The Arunta Inlier; a complex ensialic mobile belt in central Australia. Part 2: tectonic history, *Australian Journal of Earth Sciences*, **31**, 457-484.
REID M. D. 2012 New constraints on Chewings-aged deformation and metamorphism of ca. ≥1750 Ma crust in the Reynolds Range, central Australia. Honours thesis. University of Adelaide, Adelaide (unpubl.).
RÖSEL D., ZACK T. & BOGER S. D. 2014 LA-ICP-MS U-Pb dating of detrital rutile and zircon from the Reynolds Range: A window into the Palaeoproterozoic tectonosedimentary evolution of the North Australian Craton, *Precambrian Research*, **255**, 381-400.
RUDNICK R. L. & GAO S. 2014 4.1 - Composition of the Continental Crust A2 - Holland, Heinrich D. In TUREKIAN K. K. ed. Treatise on Geochemistry (Second Edition). pp. 1-51. Oxford: Elsevier.
SANDIFORD M., MCLAREN S. & NEUMANN N. 2002 Long-term thermal consequences of the redistribution of heat-producing elements associated with large-scale granitic complexes, *Journal of Metamorphic Geology*, **20**, 87-98.
SCRIMGEOUR I. 2013 Chapter 12: Aileron Province: in Ahmad M and Munson TJ(compilers). ' Geology and mineral resources of the Northern Territory', *Northern Territry Geological Survey*, **Special Publication**.
SCRIMGEOUR I. R. 2003 Develpoing a revised framework for the Aurnta region, *Geological Survey Record*, **1**, 01-03.
SCRIMGEOUR I. R., KINNY P. D., CLOSE D. F. & EDGOOSE C. 2005 High-T grnulites and polymetamorphism in the southern Arunta region, central Australia; evidence fro a 1.64 Ga accretinal event, *Precambrian Research*, **142**, 1-27.
SHAND S. J. 1943 Eruptive Rocks. Their Genesis, Composition, Classification, and Their Relation to Ore-Deposits with a Chapter on Meterorite., *New Yorck: John Wiler & Sons*.
SLÁMA J., KOŠLER J., CONDON D. J., CROWLEY J. L., GERDES A., HANCHAR J. M., HORSTWOOD M. S., MORRIS G. A., NASDALA L. & NORBERG N. 2008. Plešovice zircon—a new natural reference material for U–Pb and Hf isotopic microanalysis. *Chemical Geology* **249**, 1-35.
STEWART A., OFFE L., GLIKSON A., WARREN R. G. & BLACK L. 1980 Geology of the northern Arunta Block, Northern Territory, *Bureau of Mineral Resources, Australia, Record*, **63**.
STEWART A. 1981 Reynolds Range region. Bureau of Mineral Resources 1:100 000 Geological Map Series. Canberra.
STEWART J. R. & BETTS P. G. 2010 Implications for Proterozoic plate margin evolution from geophysical analysis and crustal-scale modeling within the western Gawler Craton, Australia, *Tectonophysics*, **483**, 151-177.
SUN S.-S., WARREN R. G. & SHAW R. D. 1995 Nd isotope study of granites from the Arunta Inlier, central Australia: constraints on geological models and limitation of the method, *Precambrian Research*, **71**, 301-314.

TAYLOR S. R. 1985 The continental crust, its composition and evolution : an examination of the geochemical record preserved in sedimentary rocks. Blackwell Scientific Publications, Oxford Melbourne.
VRY J., COMPSTON W. & CARTWIRGHT I. 1996 SHRIMP II dating of zircons and moazites; reassessing the timing of high-grade metamorphism and fluid flow in the reynold Ranges, northern Arunta Block, Australia, *Journal of Metamorphic Geology*, **14**, 335-350.
WADE B. P., BAROVICH K. M., HAND M., SCRIMGEOUR I. R. & CLOSE D. F. 2006 Evidence for Early Mesoproterozoic Arc Magmatism in the Musgrave Block, Central Australia: Implications for Proterozoic Crustal Growth and Tectonic Reconstructions of Australia, *The Journal of Geology*, **114**, 43-63.
WARK D. A. & MILLER C. F. 1993 Accessory mineral behavior during differentiation of a granite suite: monazite, xenotime and zircon in the Sweetwater Wash Pluton, southeastern California, U.S.A. In WATSON E. B., HARRISON T. M., MILLER C. F. & RYERSON F. J. eds. pp. 49-67. Amsterdam: Amsterdam, Netherlands: Elsevier.
WATSON E. B. & HARRISON T. M. 1983 Zircon saturation revisited: temperature and composition effects in a variety of crustal magma types, *Earth and Planetary Science Letters*, **64**, 295-304.
WATT G. R. & HARLEY S. L. 1993 Accessory phase controls on the geochemistry of crustal melt and restites produced during water-undersaturated partial melting, *Contributions to Mineralogy and Petrology*, **114**, 550-566.
WEDEPOHL K. H. 1995 The composition of the continental crust, *Geochimica et cosmochimica Acta*, **59**, 1217-1232.
WEILL D. F. & DRAKE M. J. 1973 Europium Anomaly in Plagioclase Feldspar: Experimental Results and Semiquantitative Model, *Science*, **180**, 1059-1060.
WONG B. L., MORRISSEY L. J., HAND M., FIELDS C. E. & KELSEY D. E. 2015 Grenvillian-aged reworking of late Paleoproterozoic crust of the southern North Australian Craton, central Australia: Implications for the assembly of Mesoproterozoic Australia, *Precambrian Research*, **270**, 100-123.
WORDEN K., CARSON C., CLOSE D. F., DONNELLAN N. & SCRIMGEOUR I. R. 2008 Summary of Results. Joint NTGS-GA geochronology: Tanami Region, Arunta Region, Pine Creek Orogen and Halls Creek Orogen correlatives, January 2005-March 2007, *Northern Territory Geological Survey Record*, **3**.
ZHAO J.-X. 1994 Geochemical and Sm-Nd isotopic study of ampibolites in the southern Arunta Inlier, central Australia: evidence for subduction at a Proterozoic continental margin, *Precambrian Research*, **65**, 71-94.
ZHAO J.-X. & BENNETT V. C. 1995 SHRIMP U・Pb zircon geochronology of granites in the Arunta Inlier, central Australia: implications for Proterozoic crustal evolution, *Precambrian Research*, **71**, 17-43.
ZHAO J.-X. & MCCULLOCH M. T. 1995 Geochemical and Nd isotopic systematics of granites from the Arunta Inlier, central Australia: implications for Proterozoic crustal evolution, *Precambrian Research*, **71**, 265-299.

APPENDIX A: SAMPLE LOCATIONS AND METHODS USED

Samples used in this study, location, rock type, and analyses.

Sample ID	Easting	Northing	rock type	Geochron	Thin Section	Geochemistry	Isotope
72921017	261723.857	7511487.528	granite			✓	✓
72921019	293924.394	7505987.497	granite			✓	
85924153	286524.201	7504287.483	microgranite			✓	✓
85924155	286524.201	7504287.483	granite (orthogneiss)			✓	
85924167	251823.637	7518787.57	granite (orthogneiss)			✓	✓
85924196	309424.654	7500787.54	granite (orthogneiss)			✓	✓
85924200	299424.485	7507387.538	granite (orthogneiss)			✓	
85924162C	277824.114	7508787.511	granite (orthogneiss)			✓	
85924163A	269723.937	7509287.582	granite (orthogneiss)			✓	
85924183A	280324.182	7513987.533	migmatitic granite			✓	
NAP2010-2	291171	7505518	microgranite		✓	✓	
NAP2010-3	283802	7507419			✓	✓	
NAP2010-4	283802	7507419	Napperby	✓	✓	✓	
NAP2010-5	283525	7507263	Weakly foliated late stage granite	✓	✓	✓	✓
NAP2010-6	283525	7507263	Napperby Gneiss wallrock to 5		✓	✓	✓
NAP2010-7	266861	7515439	Migmatised Napperby Gneiss		✓	✓	✓
NAP2010-8	266861	7515439	Migmatised Napperby Gneiss		✓	✓	
NAP2010-9	266861	7515439	Migmatised Napperby Gneiss		✓	✓	
NAP2010-10	266861	7515439	Even grained granite	✓	✓		
NAP2010-11	259896	7511348	granite (orthogneiss)		✓	✓	
NAP2010-12	259896	7511348	granite (orthogneiss)		✓	✓	
NAP2010-13	259896	7511348					

NAP2012-2			Leucosome				
NAP2012-3	291163	7505462	Mylonite				
NAP2012-4	291187	7505425	granite (orthogneiss)		✓	✓	
NAP2012-6	294048	7505815	granite (orthogneiss)		✓	✓	
NAP2012-8	340887	7498589	granite (orthogneiss)		✓	✓	
NAP2012-10	304921	7498612	granite (orthogneiss)	✓	✓	✓	
NAP2012-11a	298804	7511258	metasedimentary raft	✓		✓	
NAP2012-12	304734	7498708	granite (orthogneiss)	✓	✓	✓	
NAP2012-13	299066	7511254	Leucosome				
NAP2012-14	298804	7511258	Leucosome				
NAP2012-15	298804	7511258	granite (orthogneiss)		✓	✓	
NAP2012-16	299824	7511466	Leucosome				

APPENDIX B: TRACE ELEMENT GEOCHEMISTRY FROM THIS STUDY

Sample ID	72921017	72921019	85924153	85924155	85924167	85924196	85924200	85924162C	85924163A	85924183A
Ag	<0.5	<0.5	<0.5	<0.5	<0.5	<0.5	<0.5	<0.5	<0.5	<0.5
As	<5	<5	<5	<5	<5	<5	<5	<5	<5	<5
Ba	550	727	221	420	630	346	630	741	543	600
Cd	<0.5	<0.5	<0.5	<0.5	<0.5	<0.5	<0.5	<0.5	<0.5	<0.5
Ce	163	115.5	287	121	126.5	72.2	92	124	161.5	100
Co	63	90	3	5	8	5	4	4	5	5
Cr	10	10	140	260	240	210	170	150	130	180
Cs	10.1	4.5	4.5	9.98	16	4.89	10.2	7.05	9.04	9.93
Cu	13	2	4	7	6	7	9	5	5	1
Dy	6.23	7.7	16.2	6.85	7.49	4.42	7	7.97	7.94	7.32
Er	2.79	4.36	8.57	3.29	4.11	3.46	4.44	4.06	3.66	3.86
Eu	1.24	1.27	0.76	0.88	1.26	0.66	1.02	1.18	1.32	1.16
Ga	21.1	18.7	21.1	18.3	18.7	17.1	18.4	17.6	20.8	19.9
Gd	9.11	8.53	19.1	8.11	9.2	3.48	6.95	8.53	9.93	7.7
Hf	7.1	6.5	11.8	7.5	7.4	5.9	5.6	6.5	11.2	8.8
Ho	1.08	1.51	3.21	1.24	1.45	0.99	1.46	1.45	1.42	1.46
La	80.9	57	131	60.6	66.6	41	45.7	58.9	81.1	48.5
Li	40	10	20	20	60	10	30	30	30	30
Lu	0.25	0.52	0.93	0.31	0.51	0.6	0.56	0.46	0.42	0.4
Mo	1	2	2	1	1	<1	<1	<1	<1	<1
Nb	18.4	12.2	29.6	16.4	14.2	7	10.8	12.1	20.8	15.8
Nd	60.3	46.1	107.5	45.9	52.6	22	36	48	60.2	39.7
Ni	7	5	3	7	9	5	4	6	6	7
Pb	44	19	56	32	30	11	27	33	32	33

Pr	17.65	12.8	31.8	12.95	14.3	6.88	9.99	13.85	17.4	11
Rb	367	224	512	395	305	168.5	344	290	360	339
Sc	8	6	6	7	11	5	6	7	8	8
Sm	11.7	9.36	23	9.19	10.1	3.75	7.26	10.25	11.55	8.28
Sn	13	7	9	9	6	5	17	6	5	14
Sr	71.6	83.6	44.7	58.7	95	186	71.5	81.9	69.3	69.2
Ta	2.8	1.4	1.4	1.3	1.4	0.7	1.5	1.2	1.8	1.4
Tb	1.25	1.35	3.05	1.23	1.33	0.6	1.08	1.37	1.42	1.23
Th	63.4	30.5	165.5	44.9	31.6	36.8	26	33.8	46.7	27.3
Tl	<10	<10	<10	<10	<10	<10	<10	<10	<10	<10
Tm	0.32	0.57	1.19	0.41	0.56	0.53	0.64	0.54	0.49	0.54
U	23	4.57	48.9	5.25	4.94	5.35	4.68	5.94	5.47	7.02
V	33	27	10	31	51	28	19	21	30	32
Y	29.6	43.6	93.1	35	40.7	30.5	42.7	41.7	38.8	40.8
Yb	1.79	3.8	6.66	2.43	3.65	3.84	4.18	3.17	2.88	2.94
Zn	64	8	53	47	62	10	30	44	64	66
Zr	246	232	388	265	275	199	194	227	399	312
Sample ID	**NAP2010-2**	**NAP2010-3**	**NAP2010-4**	**NAP2010-5**	**NAP2010-6**	**NAP2010-7**	**NAP2010-8**	**NAP2010-9**	**NAP2010-11**	**NAP2010-12**
Ag	<0.5	<0.5	<0.5	<0.5	<0.5	<0.5	<0.5	<0.5	<0.5	<0.5
As	<5	<5	<5	<5	<5	<5	<5	<5	<5	<5
Ba	203	588	606	329	695	724	692	610	679	664
Cd	<0.5	<0.5	<0.5	<0.5	<0.5	<0.5	<0.5	<0.5	<0.5	<0.5
Ce	120	107.5	105.5	141	122	136.5	91.5	83.7	99	101
Co	23	26	25	25	18	30	28	25	31	18
Cr	20	10	10	<10	10	10	10	10	20	20
Cs	2.91	1.59	3.03	2.04	5.51	8.8	7.92	8.81	12.9	12.25
Cu	2	2	3	3	1	14	33	11	10	18

Dy	7.01	6.37	6.84	8.71	7.62	9.1	5.68	8.96	6.89	7.18
Er	3.77	3.54	3.85	3.69	4.01	5.05	2.67	6.27	3.89	4.49
Eu	0.93	1.01	1	0.84	1.03	1.25	1.06	1.17	1.38	1.11
Ga	14.4	17.7	18.5	19	17.8	18.8	19.2	25.5	19.9	18
Gd	8.01	7.19	7.46	10.45	8.45	9.78	7.25	8.11	7.42	6.92
Hf	6.5	6	5.7	5.3	6	6.2	5.2	5	7	6.1
Ho	1.31	1.2	1.32	1.48	1.4	1.73	1.02	1.98	1.41	1.51
La	58.7	54.5	52.5	70.4	59.9	67.4	44.6	41.2	51.3	43.9
Li	20	10	10	10	30	30	30	40	40	40
Lu	0.47	0.44	0.48	0.34	0.44	0.65	0.32	0.95	0.48	0.59
Mo	<1	1	<1	<1	<1	<1	<1	<1	<1	<1
Nb	11.4	9.9	13.3	11.8	13.3	15.6	12.2	13.8	15.7	12.7
Nd	46.2	41.5	42.1	51.3	48.1	53	35.9	33.4	39.6	35.4
Ni	5	6	5	1	4	4	3	3	8	7
Pb	16	22	25	70	31	34	36	42	33	35
Pr	12.6	11.3	11.4	14.9	13.4	14.25	9.88	9.14	10.95	9.64
Rb	152.5	193	204	408	336	324	341	350	365	350
Sc	5	5	6	3	5	6	4	5	11	11
Sm	9.79	8.06	8.28	11.2	9.66	10.85	7.89	7.85	7.93	7
Sn	8	6	8	7	8	9	8	9	11	10
Sr	84.1	75.5	77.4	54.5	66.4	67.4	58.6	66.6	101.5	89.6
Ta	1.4	1	1.3	0.6	1.2	1.5	1.1	1.3	1.9	1.3
Tb	1.2	1.06	1.13	1.67	1.31	1.57	1.11	1.42	1.17	1.13
Th	27.5	27.4	28	79.5	37.5	36.5	28.1	26.4	24.8	27.4
Tl	<10	<10	<10	<10	<10	<10	<10	<10	<10	<10
Tm	0.52	0.47	0.51	0.45	0.52	0.68	0.35	0.96	0.55	0.64
U	4.34	4	4.63	7.76	3.21	5.07	4.92	7.4	4.19	4.29

V	23	21	28	7	17	23	14	16	47	45
Y	37.1	35	37.3	45.9	39.1	50.9	29.1	55.5	40.4	44.2
Yb	3.3	3.11	3.5	2.59	3.17	4.37	2.36	6.57	3.32	4.11
Zn	16	12	22	32	36	53	38	42	60	59
Zr	229	218	210	155	213	226	168	165	264	232

Sample ID	**NAP2012-4**	**NAP2012-6**	**NAP2012-8**	**NAP2012-10**	**NAP2012-11a**	**NAP2012-12**	**NAP2012-15**
Ag	<0.5	<0.5	<0.5	<0.5	<0.5	<0.5	<0.5
As	<5	<5	<5	<5	<5	<5	<5
Ba	727	763	897	1050	828	379	738
Cd	<0.5	<0.5	<0.5	<0.5	<0.5	<0.5	<0.5
Ce	117.5	103.5	60.7	94.5	147.5	148.5	101
Co	28	33	21.2	31	36	31	31.5
Cr	10	10	10	10	110	10	10
Cs	12.15	2.24	1.3	6.38	11.7	3.79	1.31
Cu	4	2	1	<1	3	1	3
Dy	6.56	7.25	7.65	7.87	5.57	11.15	8.96
Er	3.56	4.06	4.41	4.29	2.58	6.1	4.5
Eu	1.2	1.17	0.8	1.23	1.38	1.35	1.15
Ga	18	18.5	16.9	19.4	28.9	18.1	17.6
Gd	7.62	7.55	6.85	8.19	7.36	11.6	8.65
Hf	5.9	9	5.2	7	5.9	8.1	6.5
Ho	1.24	1.43	1.57	1.69	0.99	2.12	1.72
La	58.7	50.7	28.2	42.9	76.3	58.7	50.3
Li	40	10	<10	30	40	30	<10
Lu	0.41	0.51	0.55	0.5	0.3	0.72	0.48
Mo	<1	<1	<1	<1	<1	1	<1

Nb	11.9	12	27	13.4	58.3	15.9	40.2
Nd	46.4	41.9	27	38.3	58.3	61	40.2
Ni	5	8	<1	5	47	5	4
Pb	29	23	12	15	8	23	27
Pr	12.8	11.2	7	10.2	15.75	16.55	10.9
Rb	341	258	201	341	258	314	209
Sc	6	6	3	5	14	6	3
Sm	9.13	8.51	6.08	9.09	9.6	12.8	8.14
Sn	7	7	7	7	4	6	5
Sr	76.7	79.9	90.8	97.7	84.9	43.3	64.1
Ta	1.3	1.1	1.8	1.5	1.4	1	0.7
Tb	1.21	1.23	1.17	1.34	1.05	1.92	1.43
Th	29.4	27.4	23.7	29.3	26.8	40.8	28.9
Tl	<10	<10	<10	<10	<10	<10	<10
Tm	0.46	0.54	0.63	0.62	0.33	0.83	0.58
U	4.64	4.63	2.86	3.95	3.85	6.95	4.86
V	26	26	7	20	108	25	19
Y	34.7	41.6	20	45	26.7	58	30
Yb	2.89	3.75	4.06	3.45	2.14	5.2	3.57
Zn	40	19	4	8	27	40	28
Zr	207	328	169	246	213	293	227

APPENDIX C: U-PB ZIRCON GEOCHRONOLOGY DATA

	Isotope Ratios				Ages				
Analysis	Pb207/U235		Pb206/U238		Pb206/U238		2Pb07/Pb206		Concordancy
NAP401	4.619	0.091	0.304	0.0047	1713	24	1789	31	96
NAP402	4.623	0.058	0.2978	0.0034	1680	17	1847	17	91
NAP411	4.38	0.064	0.2888	0.0035	1635	17	1780	25	92
NAP412	4.19	0.058	0.2826	0.0034	1604	17	1738	28	92
NAP415	4.29	0.06	0.2897	0.0036	1640	18	1760	26	93
NAP416	4.346	0.079	0.2923	0.0052	1652	26	1759	26	94
NAP417	4.281	0.083	0.2908	0.0049	1648	25	1770	35	93
NAP418	5.181	0.073	0.3207	0.0047	1792	23	1907	23	94
NAP419	4.156	0.059	0.2802	0.0035	1595	18	1751	22	91
NAP420	4.3	0.082	0.2881	0.0039	1631	20	1775	34	92
NAP424	5.458	0.078	0.3376	0.0042	1874	20	1918	23	98
NAP426	5.41	0.12	0.331	0.0067	1843	32	1940	33	95
NAP427	7.508	0.097	0.3756	0.0048	2055	23	2281	19	90
NAP429	4.213	0.064	0.2879	0.0035	1630	18	1713	29	95
NAP432	4.326	0.075	0.2921	0.0041	1651	20	1733	33	95
NAP436	6.85	0.11	0.3709	0.0049	2032	23	2148	25	95
NAP437	4.92	0.097	0.3072	0.0042	1726	20	1914	35	90
NAP438	4.26	0.059	0.287	0.0035	1631	17	1744	18	94
NAP444	4.721	0.068	0.3175	0.0041	1777	20	1767	23	101
NAP445	4.896	0.076	0.3097	0.0048	1738	24	1875	20	93
NAP447	5.175	0.085	0.3259	0.0042	1820	21	1864	23	98
NAP450	4.526	0.05	0.306	0.003	1722	15	1742	18	99
NAP451	4.365	0.058	0.2926	0.0038	1655	19	1770	27	94
NAP452	5.054	0.061	0.3134	0.0037	1757	18	1892	21	93
NAP454	4.792	0.089	0.2992	0.0041	1689	20	1859	30	91
NAP455	4.49	0.067	0.3086	0.0044	1732	22	1725	26	100
NAP456	4.522	0.076	0.3032	0.0042	1706	21	1753	30	97
NAP457	5.265	0.096	0.3171	0.0052	1775	25	1938	33	92
NAP458	4.356	0.074	0.302	0.0051	1700	25	1715	28	99
NAP461	4.835	0.066	0.3198	0.0039	1788	19	1784	18	100
NAP462	4.56	0.063	0.3099	0.004	1739	20	1722	24	101
NAP464	4.842	0.086	0.3218	0.0045	1799	22	1788	32	101
NAP465	4.679	0.073	0.3183	0.0042	1780	20	1727	24	103
NAP466	4.736	0.079	0.3181	0.0048	1781	24	1750	26	102
NAP467	4.513	0.091	0.2941	0.0057	1661	28	1843	34	90
NAP469	7.89	0.1	0.3958	0.0051	2149	24	2267	21	95
NAP471	3.837	0.041	0.2785	0.0028	1583	14	1607	17	99
NAP472	4.349	0.077	0.287	0.0049	1626	24	1793	27	91

	Isotope Ratios				Ages				
Analysis	Pb207/U235		Pb206/U238		Pb206/U238		2Pb07/Pb206		Concordancy
NAP473	12.58	0.15	0.4965	0.0056	2600	24	2665	13	98
NAP474	4.418	0.07	0.2935	0.0047	1658	23	1777	20	93
NAP476	8.8	0.16	0.4195	0.006	2259	27	2357	23	96
NAP477	4.596	0.071	0.3105	0.0039	1745	20	1745	25	100
NAP478	4.684	0.081	0.3165	0.005	1771	24	1744	34	102
NAP481	4.592	0.069	0.311	0.0039	1746	19	1749	29	100
NAP484	4.894	0.058	0.3307	0.0034	1841	16	1744	18	106
NAP485	4.289	0.07	0.2874	0.005	1630	25	1786	29	91
NAP486	13.1	0.18	0.519	0.0062	2695	26	2661	14	101
NAP487	11.06	0.13	0.4828	0.006	2538	26	2512	16	101
NAP488	4.803	0.069	0.3185	0.0043	1781	21	1774	28	100
NAP493	4.507	0.058	0.3103	0.0042	1741	21	1709	30	102
NAP501	5.27	0.11	0.3299	0.0049	1837	24	1896	27	97
NAP502	5.128	0.059	0.3405	0.0034	1888	16	1797	18	105
NAP503	4.81	0.065	0.3195	0.0036	1787	17	1775	25	101
NAP505	4.719	0.072	0.3016	0.004	1698	20	1859	16	91
NAP506	5.7	0.065	0.3508	0.0041	1937	19	1951	22	99
NAP507	5	0.13	0.3203	0.0056	1789	27	1853	22	97
NAP509	5.122	0.075	0.3218	0.0041	1797	20	1882	22	95
NAP514	3.675	0.052	0.2626	0.0033	1504	17	1644	17	91
NAP515	4.62	0.057	0.3051	0.0037	1716	18	1789	20	96
NAP516	4.477	0.057	0.299	0.0037	1686	18	1768	20	95
10A002	4.234	0.064	0.2908	0.0053	1644	27	1730	29	95
10A005	4.65	0.076	0.3119	0.006	1748	29	1757	28	99
10A006	4.374	0.088	0.2995	0.0052	1690	25	1752	33	96
10A008	4.409	0.077	0.2955	0.0047	1667	24	1753	24	95
10A011	4.343	0.089	0.2858	0.0046	1619	23	1795	29	90
10A017	4.011	0.079	0.2756	0.0043	1568	22	1718	24	91
10A021	4.66	0.083	0.3123	0.0057	1750	28	1755	26	100
10A022	4.314	0.083	0.2995	0.0064	1687	32	1710	35	99
10A024	4.56	0.078	0.3117	0.0054	1750	27	1729	33	101
10A027	4.554	0.08	0.3083	0.0054	1733	26	1750	29	99
10A028	4.503	0.066	0.3043	0.0048	1711	24	1747	27	98
10A029	4.439	0.077	0.3047	0.0053	1715	26	1740	34	99
10A031	4.641	0.092	0.313	0.0058	1754	29	1742	32	101
10A032	4.471	0.084	0.3056	0.0052	1717	26	1757	34	98
10A033	5.447	0.093	0.3406	0.0057	1888	28	1918	19	98
10A038	4.02	0.068	0.296	0.0049	1673	24	1591	29	105

	Isotope Ratios				Ages				
Analysis	Pb207/U235		Pb206/U238		Pb206/U238		2Pb07/Pb206		Concordancy
10A043.D	4.602	0.088	0.3112	0.0057	1747	28	1767	23	99
10A044.D	4.907	0.082	0.3244	0.0051	1809	25	1782	24	102
10A046.D	4.751	0.082	0.3172	0.0055	1778	26	1745	26	102
10A047.D	7.82	0.12	0.4018	0.0055	2176	25	2253	25	97
10A048.D	4.395	0.068	0.3014	0.005	1699	24	1704	28	100
10A050.D	4.749	0.083	0.3133	0.0047	1756	23	1791	24	98
10A051.D	4.565	0.095	0.3055	0.005	1720	25	1767	31	97
10A052.D	4.702	0.075	0.3143	0.005	1762	25	1744	27	101
10A053.D	4.836	0.084	0.318	0.0051	1783	25	1802	28	99
10A054.D	4.712	0.087	0.3195	0.0055	1788	26	1752	29	102
10A055.D	4.515	0.087	0.2943	0.0051	1662	25	1810	25	92
10A056.D	3.822	0.071	0.271	0.0046	1544	23	1670	30	92
10A057.D	4.744	0.082	0.3182	0.0048	1780	23	1766	28	101
10A059.D	4.826	0.08	0.3212	0.0053	1796	26	1787	29	101
10A060.D	4.458	0.074	0.2988	0.0047	1687	23	1756	21	96
10A061.D	4.647	0.067	0.3173	0.0047	1775	23	1739	24	102
10A062.D	5.17	0.1	0.3306	0.0055	1839	27	1855	31	99
10A063.D	4.873	0.087	0.3224	0.0052	1804	25	1785	24	101
10A065.D	4.7	0.1	0.3117	0.0051	1747	25	1770	28	99
10A067.D	13.7	0.25	0.5288	0.0093	2732	39	2727	27	100
10A070.D	11.46	0.23	0.46	0.0086	2437	38	2644	25	92
10A077.D	5.13	0.093	0.3302	0.0059	1841	28	1831	30	101
10A082.D	5.258	0.09	0.3248	0.0052	1812	25	1910	27	95
10A085.D	4.252	0.092	0.2826	0.005	1608	25	1754	31	92
12A003.D	10.14	0.12	0.4333	0.0059	2320	26	2559	22	91
12A004.D	3.319	0.061	0.248	0.0038	1428	19	1552	27	92
12A005.D	4.249	0.078	0.2836	0.0042	1608	21	1771	34	91
12A006.D	4.172	0.07	0.2829	0.0042	1605	21	1752	33	92
12A007.D	4.34	0.052	0.2854	0.0038	1618	19	1786	21	91
12A010.D	5.097	0.082	0.3266	0.0044	1821	21	1852	22	98
12A013.D	4.356	0.07	0.2904	0.0042	1642	21	1791	27	92
12A016.D	4.447	0.066	0.2948	0.0043	1665	22	1775	25	94
12A018.D	4.515	0.078	0.2983	0.0044	1684	22	1785	35	94
12A020.D	4.422	0.056	0.2937	0.0036	1659	18	1778	23	93
12A021.D	4.144	0.076	0.2791	0.0045	1586	23	1757	30	90
12A024.D	4.48	0.078	0.302	0.0038	1701	19	1735	29	98
12A025.D	4.53	0.063	0.3015	0.004	1700	20	1780	29	96
12A028.D	4.456	0.082	0.2994	0.0041	1690	20	1758	32	96

	Isotope Ratios				Ages				
Analysis	Pb207/U235		Pb206/U238		Pb206/U238		2Pb07/Pb206		Concordancy
12A029.D	4.444	0.081	0.2966	0.0048	1673	24	1777	33	94
12A031.D	4.702	0.074	0.3135	0.0044	1757	22	1754	29	100
12A032.D	4.7	0.1	0.3146	0.0059	1762	29	1760	35	100
12A033.D	4.531	0.066	0.3091	0.005	1735	24	1733	26	100
12A034.D	4.463	0.085	0.3071	0.0039	1728	19	1756	31	98
12A039.D	4.238	0.081	0.2921	0.0043	1654	21	1707	30	97
12A041.D	4.554	0.079	0.3124	0.0049	1751	24	1748	29	100
12A044.D	4.548	0.089	0.3076	0.0045	1728	22	1740	32	99
12A046.D	4.68	0.077	0.3161	0.0042	1772	21	1752	28	101
12A047.D	4.022	0.056	0.2769	0.004	1575	20	1712	18	92
12A048.D	4.742	0.075	0.3163	0.005	1773	24	1775	28	100
12A052.D	4.476	0.066	0.2954	0.0041	1670	21	1787	19	93
12A054.D	4.512	0.075	0.3054	0.0041	1717	20	1761	32	98
12A056.D	5.208	0.071	0.3334	0.0043	1854	21	1834	23	101
12A057.D	8.54	0.11	0.4244	0.0056	2279	25	2298	18	99
12A058.D	8.92	0.17	0.4248	0.0068	2280	31	2344	23	97
12A059.D	5.881	0.09	0.3515	0.0045	1941	21	1965	23	99
12A060.D	4.647	0.069	0.3117	0.0041	1748	20	1767	26	99
12A062.D	4.714	0.066	0.3176	0.0041	1777	20	1760	26	101
12A063.D	4.702	0.079	0.307	0.005	1728	25	1788	29	97
12A066.D	3.845	0.063	0.28	0.0038	1591	19	1607	29	99
12A067.D	5.776	0.066	0.3512	0.0045	1939	21	1927	17	101
12A068.D	4.773	0.079	0.318	0.0045	1781	22	1761	28	101
12A069.D	8.04	0.11	0.4075	0.0056	2205	25	2248	17	98
12A071.D	4.923	0.084	0.3352	0.0051	1862	25	1732	26	108
12A072.D	4.95	0.1	0.3307	0.0052	1842	25	1759	34	105
12A073.D	10.57	0.18	0.473	0.0071	2494	31	2484	32	100
12A074.D	4.971	0.073	0.3244	0.005	1810	24	1819	19	100
12A075.D	4.857	0.08	0.3218	0.0047	1799	23	1783	32	101
12A076.D	11.99	0.14	0.4834	0.0056	2547	25	2646	12	96
12A078.D	4.623	0.069	0.3043	0.0041	1711	20	1795	25	95
12A079.D	4.917	0.086	0.3263	0.0054	1821	27	1782	28	102
12A080.D	4.978	0.074	0.328	0.0052	1832	25	1785	31	103
12A082.D	4.728	0.062	0.3188	0.0042	1785	20	1746	23	102
12A083.D	4.945	0.074	0.3297	0.0044	1838	21	1768	22	104
12A087.D	5.48	0.085	0.3423	0.0052	1899	25	1909	22	99
12A088.D	4.827	0.055	0.3253	0.004	1815	19	1749	15	104
12A089.D	4.718	0.099	0.3132	0.0062	1755	30	1765	35	99

	Isotope Ratios				Ages				
Analysis	Pb207/U235		Pb206/U238		Pb206/U238		2Pb07/Pb206		Concordancy
N124102.D	6.44	0.52	0.3906	0.034	2123	160	1930	27	110
N124103.D	5.084	0.42	0.3438	0.031	1903	150	1739	32	109
N124104.D	5.01	0.41	0.3256	0.028	1815	140	1804	30	101
N124105.D	4.422	0.37	0.2941	0.026	1663	130	1763	26	94
N124106.D	4.622	0.38	0.299	0.026	1685	130	1831	20	92
N124109.D	4.643	0.38	0.3142	0.028	1759	140	1744	33	101
N124113.D	7.202	0.59	0.3843	0.034	2094	160	2158	17	97
N124116.D	4.513	0.37	0.299	0.027	1685	130	1767	26	95
N124117.D	4.531	0.37	0.3062	0.027	1721	130	1736	27	99
N124118.D	4.711	0.38	0.309	0.027	1735	130	1785	22	97
N124126.D	4.454	0.37	0.2956	0.026	1668	130	1766	30	94
N124127.D	3.789	0.31	0.2652	0.023	1516	120	1681	19	90
N124128.D	4.18	0.34	0.2825	0.025	1603	130	1737	26	92
N124131.D	4.534	0.37	0.3043	0.027	1711	130	1748	22	98
N124132.D	4.626	0.38	0.3057	0.027	1718	130	1777	28	97
N124133.D	4.352	0.36	0.2964	0.026	1672	130	1731	31	97
N124136.D	4.969	0.4	0.3207	0.028	1796	140	1813	17	99
N124140.D	4.591	0.38	0.2964	0.026	1672	130	1818	29	92
N124143.D	4.604	0.38	0.3084	0.027	1731	140	1757	34	99
N124144.D	4.519	0.38	0.3081	0.027	1730	130	1721	30	101
N124145.D	4.625	0.38	0.3063	0.027	1721	130	1774	27	97
N124146.D	4.529	0.37	0.3011	0.027	1696	130	1769	24	96
N124147.D	4.522	0.38	0.3015	0.027	1697	130	1761	30	96
N124148.D	4.463	0.37	0.3016	0.027	1701	130	1735	29	98
N124149.D	4.394	0.36	0.3013	0.027	1696	130	1718	27	99
N124150.D	4.496	0.37	0.2993	0.027	1686	130	1768	25	95
N124152.D	4.226	0.35	0.29	0.026	1640	130	1711	26	96
N124158.D	3.848	0.31	0.2683	0.023	1531	120	1696	23	90
N124159.D	5.407	0.45	0.329	0.029	1832	140	1928	28	95
N124160.D	4.937	0.41	0.3162	0.028	1770	140	1842	29	96
N124161.D	4.926	0.39	0.3138	0.027	1758	130	1847	24	95
N124162.D	4.895	0.41	0.3249	0.029	1815	140	1763	27	103
N124163.D	5.187	0.42	0.3185	0.028	1781	140	1915	21	93
N124164.D	4.787	0.4	0.32	0.028	1788	140	1755	35	102
N124166.D	5.074	0.42	0.3276	0.029	1825	140	1821	23	100
N124167.D	4.783	0.4	0.3146	0.028	1762	140	1802	21	98
N124170.D	4.714	0.39	0.3171	0.028	1777	140	1744	31	102
N124172.D	4.684	0.39	0.3136	0.028	1757	140	1766	30	99
N124173.D	6.11	0.52	0.3601	0.032	1980	150	1980	32	100
N124203.D	5.13	0.16	0.3299	0.01	1837	49	1828	30	100

	Isotope Ratios				Ages				
Analysis	Pb207/U235		Pb206/U238		Pb206/U238		2Pb07/Pb206		Concordancy
N124209.D	4.221	0.13	0.2871	0.0089	1626	45	1730	31	94
N124213.D	4.848	0.14	0.3097	0.0094	1738	46	1846	30	94
N124217.D	4.821	0.15	0.3134	0.0094	1756	46	1808	26	97
N124218.D	4.387	0.15	0.298	0.0099	1679	49	1732	34	97
N124220.D	4.791	0.15	0.3103	0.0093	1744	47	1814	25	96
N124221.D	5.26	0.17	0.3254	0.01	1814	49	1902	31	95
N124222.D	4.761	0.15	0.3135	0.0095	1757	47	1790	30	98
N124224.D	4.492	0.14	0.2992	0.0091	1689	46	1758	33	96
N124225.D	4.546	0.14	0.3081	0.0094	1731	46	1736	30	100
N124226.D	4.579	0.15	0.3068	0.0097	1723	48	1754	32	98
N124228.D	4.412	0.14	0.2921	0.009	1654	45	1768	31	94
N124229.D	4.638	0.14	0.3121	0.0095	1750	47	1746	30	100
N124231.D	4.694	0.14	0.3133	0.0095	1756	47	1763	30	100
N124232.D	4.53	0.14	0.3067	0.0095	1723	47	1737	32	99
N124234.D	4.603	0.14	0.3135	0.0096	1757	47	1734	33	101
N124239.D	4.735	0.14	0.3169	0.0096	1773	47	1758	30	101
N124240.D	4.638	0.14	0.3161	0.0098	1770	48	1727	30	102
N124241.D	11.63	0.35	0.4632	0.014	2452	63	2661	22	92
N124242.D	5.733	0.18	0.3577	0.011	1970	51	1884	29	105
N124243.D	4.74	0.15	0.318	0.0099	1778	48	1751	34	102
N124248.D	4.893	0.15	0.3155	0.0097	1766	47	1820	31	97
N124249.D	4.556	0.14	0.3077	0.0096	1728	48	1748	33	99
N124253.D	4.595	0.14	0.308	0.0097	1729	48	1755	32	99
N124258.D	4.556	0.14	0.3093	0.0093	1736	46	1734	26	100
N124259.D	4.554	0.14	0.3024	0.0093	1704	47	1769	31	96
N124262.D	5.066	0.072	0.3305	0.005	1840	24	1845	20	100
N124263.D	4.583	0.073	0.3114	0.0065	1750	31	1749	26	100
N124264.D	4.575	0.077	0.3113	0.0056	1746	28	1732	26	101
N124265.D	4.553	0.068	0.3099	0.0053	1742	26	1745	26	100
N124266.D	4.314	0.085	0.2999	0.0046	1694	23	1772	27	96
N124268.D	6.99	0.12	0.3848	0.0071	2097	33	2127	23	99
N124271.D	4.586	0.077	0.3117	0.0053	1751	27	1755	31	100
N124276.D	8.76	0.14	0.4304	0.0068	2306	30	2336	28	99
N124278.D	4.363	0.087	0.3022	0.0057	1700	28	1695	35	100
N124279.D	8.84	0.16	0.4336	0.0084	2324	37	2340	25	99
N124280.D	4.496	0.055	0.3067	0.0045	1726	23	1745	22	99
N124281.D	4.087	0.049	0.2906	0.0044	1643	22	1670	16	98
N124283.D	4.323	0.062	0.3029	0.0046	1705	23	1735	30	98
N124301.D	5.3	0.11	0.336	0.007	1866	34	1943	34	96
N124306.D	4.506	0.063	0.3062	0.0042	1721	21	1771	21	97

	Isotope Ratios				Ages				
Analysis	Pb207/U235		Pb206/U238		Pb206/U238		2Pb07/Pb206		Concordancy
N124308.D	9.34	0.13	0.4316	0.0066	2315	29	2447	21	95
N124309.D	4.731	0.082	0.3158	0.0063	1771	30	1788	33	99
N124313.D	4.57	0.08	0.3058	0.005	1719	25	1769	33	97
N124316.D	4.44	0.072	0.3062	0.0055	1720	27	1714	26	100
N124317.D	5.168	0.076	0.3313	0.0052	1843	25	1854	25	99
N124318.D	4.735	0.059	0.3147	0.0043	1763	21	1775	20	99
N124319.D	4.626	0.077	0.3135	0.0049	1756	24	1752	29	100
N124322.D	5.268	0.071	0.3343	0.005	1858	24	1864	27	100
N124325.D	4.237	0.079	0.2794	0.0051	1590	25	1763	30	90
N124327.D	4.737	0.082	0.315	0.0051	1764	25	1779	25	99
N124328.D	4.934	0.075	0.3231	0.0057	1807	27	1826	24	99
N124329.D	4.646	0.073	0.3101	0.005	1741	25	1831	29	95
N124330.D	4.943	0.088	0.3255	0.0048	1816	23	1822	28	100
N124332.D	4.643	0.072	0.3142	0.0063	1760	31	1779	32	99
N124333.D	4.806	0.083	0.3196	0.006	1786	29	1796	24	99
N124335.D	4.828	0.071	0.3203	0.0054	1790	26	1799	29	99
N124337.D	4.362	0.068	0.304	0.0047	1710	23	1708	23	100
N124338.D	8.64	0.12	0.4307	0.007	2307	32	2288	18	101
N124339.D	4.871	0.085	0.3166	0.0046	1775	22	1813	29	98
N124341.D	4.85	0.077	0.3196	0.0048	1792	24	1779	23	101
N124343.D	4.687	0.078	0.3152	0.0058	1767	29	1743	30	101
N124345.D	6.07	0.12	0.3627	0.0081	1991	39	1965	25	101
N124346.D	4.531	0.076	0.3088	0.0054	1734	26	1784	28	97
N124350.D	5.261	0.065	0.335	0.0067	1870	32	1856	26	101
N124353.D	4.851	0.083	0.3219	0.0055	1797	27	1751	27	103
N124354.D	4.836	0.088	0.3208	0.0059	1792	29	1762	27	102
N124402.D	8.64	0.11	0.4174	0.0054	2248	24	2330	19	96
N124404.D	4.576	0.064	0.3068	0.0049	1724	24	1761	30	98
N124408.D	4.573	0.076	0.3094	0.0049	1736	24	1726	28	101
N124410.D	4.385	0.064	0.2984	0.0041	1682	20	1732	23	97
N124411.D	4.001	0.062	0.2772	0.0041	1577	21	1693	20	93
N124413.D	4.471	0.062	0.3022	0.0036	1701	18	1755	24	97
N124416.D	5.068	0.053	0.323	0.0034	1803	17	1845	15	98
N124417.D	5.901	0.069	0.3522	0.0055	1944	26	1977	23	98
N124419.D	4.388	0.074	0.3015	0.0039	1698	19	1716	29	99
N124420.D	4.392	0.066	0.2992	0.0041	1686	20	1748	26	96
N124424.D	4.272	0.074	0.2896	0.0041	1638	20	1769	31	93
N124425.D	4.332	0.054	0.2993	0.0036	1687	18	1722	25	98
N124429.D	4.436	0.058	0.2989	0.0041	1684	21	1758	21	96
N124432.D	4.526	0.06	0.3045	0.0034	1713	17	1755	23	98

	Isotope Ratios				Ages				
Analysis	Pb207/U235		Pb206/U238		Pb206/U238		2Pb07/Pb206		Concordancy
11A101.D	4.988	0.083	0.3224	0.0046	1802	22	1831	19	98
11A102.D	4.363	0.05	0.3011	0.0031	1696	15	1715	16	99
11A103.D	12.04	0.22	0.4761	0.0065	2508	29	2674	18	94
11A104.D	11.663	0.094	0.4808	0.004	2530	17	2602	12	97
11A105.D	5.438	0.055	0.3386	0.0033	1881	16	1912	17	98
11A106.D	11.06	0.17	0.4768	0.0072	2516	32	2533	23	99
11A107.D	7.441	0.094	0.3977	0.0048	2157	22	2182	15	99
11A108.D	5.384	0.053	0.3322	0.0033	1851	16	1899	14	97
11A109.D	7.292	0.092	0.3838	0.0042	2093	19	2197	14	95
11A110.D	10.2	0.16	0.4598	0.0066	2441	28	2462	26	99
11A111.D	4.758	0.08	0.3174	0.0042	1776	20	1757	21	101
11A112.D	5.762	0.066	0.3479	0.0034	1925	16	1955	14	98
11A113.D	7.118	0.077	0.3807	0.0039	2080	18	2175	16	96
11A114.D	7.594	0.07	0.3957	0.004	2148	18	2214	14	97
11A115.D	6.293	0.069	0.3651	0.0042	2005	20	2030	16	99
11A116.D	5.142	0.069	0.3318	0.0038	1846	18	1847	20	100
11A117.D	8.52	0.11	0.4252	0.0043	2286	20	2284	19	100
11A118.D	8.031	0.086	0.4069	0.0039	2200	18	2268	15	97
11A119.D	7.13	0.13	0.3879	0.006	2116	29	2128	35	99
11A120.D	9.48	0.11	0.4437	0.005	2369	22	2401	14	99
11A121.D	6.783	0.063	0.3879	0.0041	2112	19	2050	13	103
11A122.D	10.95	0.11	0.4823	0.0047	2538	20	2515	15	101
11A123.D	10.63	0.12	0.4739	0.005	2502	22	2474	18	101
11A124.D	12.1	0.21	0.4999	0.0079	2610	34	2626	19	99
11A125.D	10.02	0.12	0.4574	0.0059	2427	26	2436	17	100
11A126.D	4.86	0.053	0.3224	0.0037	1802	18	1800	15	100
11A128.D	5.382	0.068	0.3461	0.0036	1919	17	1858	22	103
11A129.D	8.96	0.11	0.4371	0.0056	2336	25	2323	19	101
11A130.D	6.707	0.073	0.383	0.0042	2089	20	2056	13	102
11A131.D	9.05	0.11	0.4406	0.0055	2352	25	2351	13	100
11A133.D	8.38	0.1	0.4136	0.0044	2232	20	2309	14	97
11A134.D	6.163	0.085	0.3653	0.0043	2008	21	1981	22	101
11A135.D	7.556	0.075	0.4121	0.0035	2224	16	2143	11	104
11A136A.D	5.923	0.068	0.3742	0.0044	2048	20	1868	11	110
11A136B.D	12.98	0.22	0.5045	0.0077	2631	33	2702	23	97
11A137.D	10.34	0.12	0.4595	0.0056	2436	25	2481	19	98
11A138.D	9.17	0.12	0.4386	0.0045	2347	20	2364	16	99
11A140.D	9	0.11	0.4388	0.0049	2346	22	2335	16	100

	Isotope Ratios				Ages				
Analysis	Pb207/U235		Pb206/U238		Pb206/U238		2Pb07/Pb206		Concordancy
11A141.D	5.155	0.048	0.322	0.0033	1799	16	1873	15	96
11A142.D	5.119	0.053	0.3222	0.0034	1800	17	1874	16	96
11A143.D	8.4	0.11	0.4098	0.0063	2216	28	2311	21	96
11A144.D	5.621	0.079	0.3298	0.0035	1836	17	1991	15	92
11A146.D	5.811	0.086	0.3467	0.005	1918	24	1950	29	98
11A147A.D	3.961	0.04	0.2807	0.0024	1594	12	1670	17	95
11A147B.D	6.013	0.081	0.344	0.0038	1905	18	2041	18	93
11A148.D	5.855	0.073	0.3455	0.0041	1912	20	1968	18	97
11A149.D	4.855	0.067	0.3081	0.0039	1731	19	1855	24	93
11A150.D	5.62	0.075	0.3434	0.004	1902	19	1908	25	100
11A151.D	5.078	0.069	0.3221	0.0045	1799	22	1857	27	97
11A152.D	4.99	0.052	0.3146	0.0031	1763	15	1848	15	95
11A153.D	4.609	0.051	0.2981	0.0026	1682	13	1805	14	93
11A154.D	6.07	0.08	0.3527	0.004	1949	19	1997	18	98
11A155.D	9.45	0.15	0.4252	0.0055	2283	25	2442	22	93
11A156.D	7.64	0.13	0.395	0.0058	2148	26	2233	22	96
11A157.D	4.915	0.074	0.317	0.0044	1774	21	1840	25	96
11A158.D	4.786	0.06	0.3112	0.0038	1748	19	1810	17	97
11A159.D	5.632	0.062	0.338	0.0035	1876	17	1954	19	96
11A160.D	10.8	0.13	0.4699	0.0054	2489	24	2498	20	100
11A161.D	7.19	0.12	0.3905	0.0052	2124	24	2125	29	100
11A162.D	10.83	0.18	0.4504	0.0066	2395	29	2599	20	92
11A163.D	12.26	0.16	0.488	0.0051	2568	23	2641	11	97
11A164.D	11.36	0.18	0.465	0.0069	2460	31	2603	24	95
11A165.D	13.09	0.11	0.5101	0.0053	2658	22	2698	12	99
11A166.D	6.053	0.079	0.3615	0.0041	1988	20	1974	12	101
11A201.D	5.525	0.06	0.3385	0.0032	1879	15	1915	16	98
11A202.D	9.67	0.12	0.4351	0.0049	2328	22	2449	14	95
11A203.D	6.227	0.071	0.3592	0.0041	1978	20	2036	16	97
11A204.D	8.68	0.16	0.4334	0.0067	2319	30	2296	28	101
11A205.D	8.06	0.11	0.3979	0.0044	2159	20	2280	17	95
11A206.D	5.963	0.081	0.3545	0.0045	1955	21	1966	20	99
11A207.D	6.99	0.074	0.376	0.0038	2057	18	2142	12	96
11A208.D	7.844	0.084	0.4051	0.0048	2192	22	2209	13	99
11A209.D	10.28	0.18	0.4448	0.0061	2371	27	2529	25	94
11A210.D	6.197	0.076	0.3627	0.0045	1996	21	2010	18	99
11A211.D	5.563	0.078	0.3441	0.0047	1906	22	1902	21	100
11A212.D	9.41	0.1	0.4301	0.0047	2307	21	2435	14	95

	Isotope Ratios				Ages				
Analysis	Pb207/U235		Pb206/U238		Pb206/U238		2Pb07/Pb206		Concordancy
11A213.D	5.239	0.066	0.3349	0.0041	1863	20	1834	22	102
11A214.D	5.338	0.071	0.3373	0.0038	1874	19	1863	18	101
11A215.D	5.33	0.068	0.3358	0.005	1868	24	1890	19	99
11A216.D	8.323	0.097	0.4019	0.0057	2177	26	2343	14	93
11A217B.D	5.65	0.1	0.3554	0.0066	1963	31	1893	23	104
11A218.D	9.43	0.14	0.4377	0.0062	2341	28	2423	30	97
11A219.D	9.16	0.11	0.4423	0.0058	2359	26	2348	22	100
11A220.D	5.802	0.054	0.351	0.0033	1939	16	1943	15	100
11A221.D	5.502	0.074	0.3388	0.0035	1880	17	1918	19	98
11A222.D	5.376	0.053	0.3362	0.0034	1870	16	1884	14	99
11A223.D	5.199	0.059	0.3324	0.0033	1851	16	1850	16	100
11A224.D	6.51	0.12	0.3808	0.0056	2078	26	2007	33	104
11A225.D	13.16	0.2	0.5064	0.007	2643	31	2709	23	98
11A226.D	9.308	0.098	0.4373	0.0052	2341	23	2385	17	98
11A227.D	6.646	0.068	0.3778	0.0041	2067	19	2052	15	101
11A228.D	5.83	0.069	0.3577	0.0039	1973	19	1902	17	104
11A230.D	5.439	0.069	0.3507	0.0048	1937	23	1841	19	105
11A231.D	5.405	0.062	0.3364	0.0039	1869	19	1892	24	99
11A232.D	6.125	0.095	0.3609	0.0047	1987	22	2000	20	99
11A233.D	7.81	0.12	0.419	0.0045	2255	20	2162	24	104
11A234.D	5.776	0.067	0.3605	0.004	1986	19	1909	14	104
11A235.D	8.61	0.11	0.4318	0.0052	2313	23	2286	14	101
11A236.D	7.89	0.12	0.4152	0.0064	2239	29	2206	14	101
11A237.D	5.723	0.069	0.3553	0.0041	1961	19	1920	15	102
11A238.D	10.313	0.091	0.4644	0.0044	2458	20	2465	12	100
11A239.D	5.723	0.073	0.3498	0.0038	1933	18	1933	21	100
11A240.D	4.915	0.064	0.319	0.0038	1784	18	1819.3	9.8	98
11A241.D	7.44	0.11	0.3928	0.0056	2135	26	2188	19	98
11A242.D	5.502	0.056	0.351	0.0034	1939	16	1872	12	104
11A243.D	6.47	0.076	0.3719	0.0037	2039	17	2067	17	99
11A244.D	5.266	0.071	0.3383	0.0041	1877	20	1860	22	101
11A247.D	5.279	0.077	0.3352	0.0041	1866	20	1864	18	100
11A248.D	11.55	0.13	0.4811	0.0059	2531	26	2591	19	98
11A249.D	6.404	0.062	0.3701	0.0041	2029	19	2030	14	100
11A250.D	5.567	0.083	0.3459	0.0049	1913	24	1919	12	100
11A251.D	11.4	0.13	0.4582	0.0046	2431	20	2641	12	92
11A252.D	6.213	0.07	0.3751	0.004	2053	19	1950	18	105
11A253.D	7.297	0.072	0.3994	0.0044	2165	20	2127	13	102

	Isotope Ratios				Ages				
Analysis	Pb207/U235		Pb206/U238		Pb206/U238		2Pb07/Pb206		Concordancy
11A321.D	5.686	0.068	0.3512	0.0041	1939	20	1919	19	101
11A322.D	6.589	0.076	0.3758	0.0043	2058	20	2050	15	100
11A323.D	5.734	0.066	0.3496	0.0039	1932	18	1933	13	100
11A325.D	7.621	0.075	0.3969	0.0046	2157	22	2204	15	98
11A326.D	7.63	0.12	0.4024	0.0054	2179	25	2189	25	100
11A327.D	6.105	0.08	0.3521	0.0037	1944	18	2033	21	96
11A328.D	7.444	0.076	0.4003	0.0041	2170	19	2146.7	9	101
11A329.D	5.063	0.049	0.328	0.0037	1828	18	1829	12	100
11A330.D	5.578	0.062	0.3406	0.0048	1891	23	1932	17	98
11A331.D	5.111	0.04	0.3219	0.0028	1798	14	1878	12	96
11A332.D	6.56	0.081	0.3706	0.0044	2032	21	2057	19	99
11A333.D	5.535	0.082	0.3389	0.0051	1882	25	1938	24	97
11A334A.D	4.861	0.061	0.3203	0.0039	1792	19	1812	13	99
11A334B.D	8.93	0.13	0.4329	0.0075	2317	34	2309	31	100
11A335.D	5.994	0.066	0.3586	0.0042	1977	20	1971	17	100
11A336.D	8.565	0.08	0.4256	0.0035	2287	16	2287	13	100
11A338.D	4.984	0.077	0.3266	0.0044	1823	21	1790	23	102
11A339.D	7.349	0.075	0.3911	0.0046	2127	21	2165	12	98
11A340.D	9.44	0.13	0.4392	0.0056	2352	26	2393	21	98
11A341.D	9.13	0.14	0.444	0.0062	2369	28	2307	20	103
11A342.D	7.418	0.085	0.3973	0.0052	2157	24	2173	13	99
11A343.D	5.292	0.083	0.338	0.0055	1880	26	1852	20	102
11A344.D	7.318	0.072	0.393	0.0037	2138	17	2161	13	99
11A345.D	6.878	0.079	0.3791	0.0046	2073	21	2105	16	98
11A346.D	9.28	0.11	0.4186	0.0045	2256	21	2456	17	92
11A347.D	10.11	0.11	0.4564	0.0052	2425	23	2444	12	99
11A348.D	5.647	0.096	0.3444	0.0053	1910	25	1921	35	99
11A349.D	5.425	0.078	0.3354	0.0051	1863	25	1912	16	97
11A350.D	5.267	0.058	0.3306	0.0045	1841	22	1889	19	97
11A351.D	9.51	0.17	0.4371	0.0075	2340	34	2421	27	97
11A352.D	8.5	0.12	0.4194	0.0059	2256	27	2305	22	98
11A353.D	10.27	0.12	0.4376	0.005	2339	22	2547	13	92
11A354.D	6.744	0.082	0.373	0.0047	2045	23	2115	23	97
11A355.D	7.966	0.073	0.4099	0.0039	2215	17	2246	15	99
11A356.D	7.2	0.087	0.3782	0.0045	2067	21	2193	16	94
11A357.D	5.404	0.049	0.339	0.0039	1883	18	1884	13	100
11A358.D	9.06	0.11	0.4401	0.0055	2350	25	2320	14	101
11A359.D	10.7	0.13	0.4717	0.0053	2490	23	2488	14	100

	Isotope Ratios				Ages				
Analysis	Pb207/U235		Pb206/U238		Pb206/U238		2Pb07/Pb206		Concordancy
11A254.D	11.47	0.14	0.4852	0.0062	2554	26	2571	19	99
11A255.D	6.46	0.13	0.3575	0.0071	1974	35	2108	18	94
11A256.D	4.827	0.094	0.3224	0.0052	1804	26	1774	30	102
11A257.D	5.272	0.051	0.3386	0.0037	1879	18	1848	11	102
11A258.D	6.092	0.083	0.3601	0.0044	1981	21	1989	12	100
11A259.D	7.362	0.099	0.3993	0.0048	2169	22	2135	16	102
11A260.D	5.597	0.078	0.3449	0.0044	1909	21	1918	15	100
11A261.D	10.48	0.11	0.4658	0.0052	2466	23	2485	16	99
11A262.D	9.6	0.11	0.4482	0.0051	2391	22	2411	14	99
11A263.D	7.95	0.12	0.41	0.006	2214	28	2246	22	99
11A264.D	5.021	0.054	0.3229	0.0044	1803	21	1832	17	98
11A266.D	6.923	0.099	0.3747	0.0049	2051	23	2157	21	95
11A267.D	7.72	0.11	0.3929	0.0061	2138	28	2249	20	95
11A268.D	10.25	0.11	0.4578	0.0053	2429	24	2463	13	99
11A269.D	6.862	0.073	0.3771	0.0047	2062	22	2137	19	96
11A270.D	7.145	0.086	0.3875	0.0039	2111	18	2154	15	98
11A271.D	4.8	0.065	0.3155	0.0035	1767	17	1808	23	98
11A272.D	9.5	0.1	0.4319	0.0045	2316	20	2448	19	95
11A301.D	8.476	0.099	0.4118	0.0046	2222	21	2327	17	95
11A302.D	7.52	0.13	0.3946	0.0055	2143	25	2195	22	98
11A303.D	5.081	0.057	0.3245	0.0036	1811	17	1854	17	98
11A304.D	5.018	0.045	0.3215	0.003	1798	15	1851	13	97
11A306.D	5.497	0.078	0.3407	0.005	1889	24	1922	23	98
11A307.D	6.076	0.087	0.3518	0.004	1943	19	2015	27	96
11A308.D	7.319	0.079	0.3798	0.0049	2075	23	2209	18	94
11A309.D	5.11	0.064	0.324	0.0033	1809	16	1867	22	97
11A310.D	5.065	0.06	0.3243	0.0037	1810	18	1862	16	97
11A311.D	7.815	0.092	0.4039	0.0043	2189	19	2229	19	98
11A312.D	13.66	0.14	0.5039	0.0062	2629	27	2790	19	94
11A313.D	8.71	0.14	0.4084	0.0061	2206	28	2412	26	91
11A314.D	4.683	0.054	0.3129	0.003	1755	15	1767	18	99
11A315.D	5.556	0.071	0.3449	0.0042	1909	20	1913	19	100
11A316.D	10.13	0.16	0.4484	0.0055	2387	24	2471	22	97
11A317.D	8.89	0.12	0.4201	0.0045	2260	20	2371	17	95
11A318.D	8.65	0.1	0.4081	0.0043	2205	20	2385	15	92
11A319.D	5.099	0.049	0.3248	0.0033	1814	16	1859	13	98
11A319.D	5.265	0.062	0.3363	0.004	1868	19	1867	18	100
11A320.D	5.242	0.072	0.3323	0.0042	1849	20	1889	15	98

	Isotope Ratios				Ages				
Analysis	Pb207/U235		Pb206/U238		Pb206/U238		2Pb07/Pb206		Concordancy
11A360.D	4.99	0.1	0.325	0.006	1822	30	1808	22	101
11A361.D	4.779	0.066	0.3178	0.0041	1781	21	1779	13	100
11A362.D	12.79	0.14	0.4974	0.0054	2602	23	2703	12	96
11A363.D	5.822	0.078	0.3524	0.0044	1947	21	1936	20	101
11A364.D	5.469	0.07	0.3413	0.0041	1894	20	1901	22	100
11A365.D	5.552	0.072	0.3432	0.0047	1903	23	1905	20	100
11A401.D	10.49	0.16	0.4379	0.0069	2345	30	2574	16	91
11A402.D	7.347	0.069	0.3969	0.0038	2154	17	2145	12	100
11A403.D	6.74	0.18	0.3806	0.0061	2078	28	2089	27	99
11A404.D	11.75	0.18	0.4916	0.0073	2577	32	2577	17	100
11A405.D	5.136	0.059	0.3307	0.0038	1846	18	1827	11	101
11A406.D	6.96	0.16	0.384	0.0064	2099	30	2112	23	99
11A407.D	5.505	0.056	0.3408	0.003	1890	14	1904	18	99
11A408.D	9.55	0.15	0.4487	0.007	2389	31	2396	19	100
11A409.D	9.79	0.15	0.4528	0.0055	2407	25	2417	18	100
11A410.D	9.22	0.11	0.4396	0.0081	2353	37	2358	32	100
11A411.D	9.39	0.19	0.4172	0.009	2250	42	2500	26	90
11A412.D	5.934	0.078	0.3516	0.0038	1942	18	1987	18	98
11A413.D	8.112	0.088	0.4169	0.0046	2245	21	2240	14	100
11A414.D	9.47	0.17	0.4463	0.0078	2378	35	2396	30	99
11A415.D	4.87	0.1	0.3214	0.0063	1795	31	1777	24	101
11A417.D	6	0.1	0.3619	0.0057	1989	27	1965	25	101
11A418.D	5.998	0.067	0.3549	0.004	1959	19	1979	23	99
11A419.D	6.322	0.085	0.3703	0.0043	2030	20	2019	19	101
11A420.D	17.62	0.23	0.5823	0.008	2964	33	2952	18	100
11A421.D	8.17	0.14	0.4167	0.0067	2243	31	2255	13	99
11A422.D	8.35	0.15	0.4209	0.0065	2263	30	2262	14	100
11A423.D	4.603	0.063	0.3085	0.0037	1733	18	1764	19	98
11A424.D	4.98	0.1	0.3237	0.0059	1805	29	1822	19	99
11A425.D	11.1	0.14	0.4802	0.0056	2527	25	2522	17	100
11A426.D	4.822	0.061	0.3204	0.0041	1791	20	1775	18	101
11A427.D	7.08	0.2	0.3883	0.0072	2115	34	2111	21	100
11A428.D	11.66	0.24	0.4744	0.0074	2501	32	2622	19	95
11A429.D	7.211	0.074	0.3916	0.0049	2129	23	2134	15	100
11A430.D	5.313	0.086	0.3361	0.0049	1867	24	1844	21	101
11A431.D	10.83	0.16	0.4702	0.0056	2483	25	2511	17	99
11A432.D	6.81	0.12	0.3827	0.006	2087	28	2080	19	100
11A433.D	6.355	0.099	0.366	0.0049	2009	23	2052	22	98

	Isotope Ratios				Ages				
Analysis	Pb207/U235		Pb206/U238		Pb206/U238		2Pb07/Pb206		Concordancy
11A434.D	4.666	0.05	0.3089	0.0038	1734	19	1787	15	97
11A435.D	6.117	0.067	0.3564	0.0039	1967	18	2013	18	98
11A436.D	5.15	0.13	0.3386	0.0053	1879	25	1795	29	105
11A437.D	6.4	0.12	0.377	0.006	2061	28	1984	18	104
11A438.D	7.3	0.14	0.3994	0.0069	2165	32	2120	20	102
11A439.D	7.29	0.14	0.3993	0.0076	2164	35	2132	21	102
11A440.D	5.773	0.08	0.3506	0.0051	1942	24	1935	17	100
11A441.D	5.69	0.11	0.3505	0.0064	1938	31	1931	19	100
11A442.D	8.7	0.16	0.4291	0.0069	2300	31	2309	21	100
11A443.D	7.56	0.12	0.4047	0.0062	2189	29	2160	11	101
11A444.D	11.19	0.13	0.4784	0.0067	2519	29	2534	14	99
11A445.D	7.426	0.088	0.391	0.0049	2127	23	2189	16	97
11A446.D	6.175	0.077	0.3653	0.0045	2008	21	1976	13	102
11A447.D	5.149	0.073	0.3315	0.0044	1844	22	1837	12	100
11A448.D	9.47	0.15	0.4465	0.0072	2377	32	2376	20	100
11A449.D	10.14	0.12	0.4602	0.0059	2439	26	2446	13	100
11A450.D	6.079	0.083	0.3595	0.0051	1983	24	1983	22	100
11A451.D	5.252	0.06	0.334	0.0039	1859	19	1848	20	101
11A452.D	7.45	0.12	0.399	0.0066	2162	30	2164	19	100
11A453.D	5.485	0.097	0.3412	0.0051	1893	24	1898	14	100
11A454.D	5.289	0.085	0.336	0.0057	1865	27	1852	13	101
11A455.D	4.854	0.063	0.3141	0.0041	1762	20	1821	13	97
11A456.D	5.332	0.085	0.3394	0.0054	1882	26	1847	15	102
11A457.D	8.18	0.11	0.4217	0.0058	2267	26	2232	17	102
11A458.D	5.437	0.086	0.3421	0.0057	1901	27	1880	16	101
11A459.D	5.873	0.081	0.3557	0.0048	1963	23	1933	17	102
11A461.D	4.9	0.11	0.3232	0.0071	1805	34	1781	26	101
11A462.D	4.103	0.06	0.294	0.0036	1662	18	1624	17	102
11A463.D	5.778	0.096	0.351	0.0052	1938	25	1936	12	100
11A464.D	5.855	0.097	0.3544	0.0052	1954	25	1933	23	101
11A465.D	10.27	0.2	0.4627	0.0087	2451	38	2454	23	100
11A466.D	5.154	0.064	0.3308	0.0045	1843	22	1854	14	99
11A467.D	12.77	0.18	0.5082	0.0076	2646	33	2660	19	99
11A468.D	4.343	0.044	0.299	0.003	1689	15	1716	19	98
11A501.D	5.206	0.084	0.3315	0.0052	1846	25	1840	20	100
11A502.D	10.2	0.17	0.4669	0.0073	2471	33	2435	15	101
11A503.D	5.72	0.091	0.3531	0.0052	1948	25	1900	13	103
11A504.D	5.271	0.071	0.3361	0.004	1869	20	1849	18	101

	Isotope Ratios				Ages				
Analysis	Pb207/U235		Pb206/U238		Pb206/U238		2Pb07/Pb206		Concordancy
11A506.D	5.131	0.079	0.3331	0.0046	1852	22	1823	20	102
11A507.D	5.46	0.075	0.3412	0.0046	1893	22	1882	19	101
11A508.D	10.88	0.13	0.4737	0.0051	2499	22	2506	14	100
11A509.D	6.105	0.085	0.3597	0.0051	1984	25	1986	17	100
11A510.D	17.88	0.31	0.592	0.011	3001	45	2969	10	101
11A511.D	4.809	0.06	0.3278	0.0041	1827	20	1721	15	106
11A512.D	5.516	0.095	0.3587	0.0059	1975	28	1797	29	110
11A514.D	8.69	0.1	0.4306	0.0061	2311	28	2298	18	101
11A515.D	4.94	0.09	0.3236	0.0057	1805	28	1821	21	99
11A516.D	5.836	0.076	0.3574	0.0047	1968	22	1924	15	102
11A517.D	5.562	0.085	0.3469	0.0049	1919	24	1877	19	102
11A518.D	5.242	0.063	0.337	0.004	1873	20	1834	16	102
11A520.D	8.69	0.11	0.4284	0.0045	2300	21	2308	15	100
11A521.D	7.7	0.12	0.4126	0.0057	2226	26	2171	16	103
11A522.D	5.366	0.064	0.3393	0.0042	1882	20	1855	14	101
11A523.D	5.07	0.1	0.3312	0.0052	1843	25	1802	20	102
11A524.D	5.469	0.089	0.3428	0.0049	1908	24	1871	22	102
11A525.D	5.766	0.08	0.3543	0.005	1956	23	1913	14	102
11A526.D	11.07	0.22	0.4788	0.0079	2526	34	2519	29	100
11A527.D	10.33	0.12	0.4661	0.0048	2465	21	2451	13	101
11A528.D	5.886	0.088	0.3577	0.0041	1971	20	1933	26	102
11A529.D	8.56	0.14	0.4245	0.0062	2282	29	2260	14	101
11A530.D	5.539	0.055	0.3299	0.0033	1837	16	1973	16	93
11A531.D	5.889	0.058	0.3574	0.0034	1969	16	1919	17	103
11A532.D	7.57	0.098	0.3994	0.0055	2165	25	2195	27	99
11A533.D	4.751	0.071	0.3133	0.0046	1756	23	1821	28	96
11A534.D	4.59	0.045	0.3125	0.0025	1752	12	1739	17	101
11A535.D	8.949	0.085	0.4217	0.0037	2269	17	2389	14	95
11A536.D	7.013	0.057	0.3886	0.0032	2116	15	2105	11	101
11A537.D	4.719	0.068	0.3137	0.0034	1758	17	1767	26	99
11A538.D	5.513	0.05	0.3386	0.0031	1879	15	1914	18	98
11A539.D	7.21	0.072	0.3815	0.0038	2084	18	2184	15	95
11A540.D	9.483	0.089	0.434	0.004	2323	18	2434	12	95
11A541.D	5.508	0.051	0.3527	0.0032	1951	15	1838	13	106
11A542.D	5.153	0.065	0.3391	0.0034	1883	16	1795	17	105
11A543.D	5.843	0.081	0.3506	0.0037	1937	18	1968	23	98
11A544.D	13.27	0.13	0.5207	0.0051	2701	22	2701	14	100
11A545.D	7.572	0.078	0.4004	0.0041	2170	19	2176	19	100

	Isotope Ratios				Ages				
Analysis	Pb207/U235		Pb206/U238		Pb206/U238		2Pb07/Pb206		Concordancy
11A546.D	6.608	0.055	0.3844	0.0035	2098	16	2024	12	104
11A547.D	6.71	0.08	0.3757	0.004	2057	19	2082	19	99
11A548.D	6.45	0.12	0.3498	0.0044	1934	21	2138	19	90
11A549.D	4.867	0.054	0.3188	0.0033	1783	16	1802	20	99
11A550.D	8.03	0.1	0.4115	0.0044	2223	20	2230	19	100
11A551.D	6.046	0.09	0.3575	0.0042	1969	20	1979	19	99
11A552.D	7.543	0.075	0.4021	0.0036	2178	17	2168	18	100
11A553.D	6.643	0.069	0.3742	0.0038	2049	18	2068	18	99
11A554.D	25.84	0.22	0.6492	0.0056	3226	22	3400	10	95
11A555.D	10.661	0.09	0.4767	0.0044	2512	19	2476	12	101
11A556.D	5.779	0.047	0.3496	0.0033	1935	16	1952	14	99
11A557.D	5.674	0.053	0.3451	0.0033	1910	16	1941	16	98
11A558.D	4.989	0.062	0.325	0.004	1815	20	1814	25	100
11A559.D	8.812	0.093	0.4279	0.0043	2297	19	2319	16	99
11A560.D	5.442	0.057	0.3359	0.0036	1866	17	1903	20	98
11A561.D	4.933	0.044	0.3192	0.0036	1785	18	1838	15	97
11A562.D	5.441	0.049	0.3441	0.0032	1906	15	1863	13	102
11A563.D	5.113	0.05	0.3305	0.0033	1840	16	1842	16	100
11A564.D	4.734	0.071	0.3102	0.0036	1741	18	1801	27	97
11A565.D	5.609	0.054	0.3474	0.0033	1922	16	1903	18	101
11A566.D	7.171	0.063	0.3849	0.0035	2102	16	2155	13	98
11A567.D	5.155	0.084	0.3236	0.0036	1807	18	1899	23	95
11A569.D	9.75	0.11	0.4467	0.0046	2380	21	2437	17	98
11A570.D	4.789	0.064	0.3102	0.0029	1743	14	1797	19	97
11A571.D	5.818	0.064	0.3557	0.0035	1964	17	1917	19	102
11A572.D	9.34	0.15	0.4382	0.0061	2343	28	2410	31	97
11A573.D	4.997	0.072	0.3234	0.0037	1806	18	1833	23	99
11A574.D	5.33	0.052	0.3349	0.0033	1863	16	1883	14	99
11A575.D	10.05	0.13	0.4494	0.0058	2392	26	2465	17	97
11A576.D	6.737	0.076	0.3713	0.004	2035	19	2112	18	96
11A577.D	5.208	0.053	0.3295	0.0036	1835	17	1862	15	99
11A578.D	5.077	0.048	0.3266	0.003	1821	14	1835	15	99
11A579.D	8.7	0.11	0.4045	0.0042	2189	19	2411	18	91
11A580.D	23.5	0.34	0.645	0.0078	3210	30	3255	14	99
11A581.D	9.9	0.12	0.4479	0.0054	2385	24	2450	18	97
11A582.D	5.184	0.056	0.3316	0.0032	1845	15	1840	16	100
11A583.D	7.382	0.075	0.3916	0.004	2130	19	2173	16	98
11A584.D	7.271	0.076	0.3873	0.0035	2109	16	2164	15	97

	Isotope Ratios				Ages				
Analysis	Pb207/U235		Pb206/U238		Pb206/U238		2Pb07/Pb206		Concordancy
11A585.D	5.052	0.079	0.3218	0.0039	1798	19	1866	31	96
11A586.D	14.07	0.24	0.5196	0.0075	2696	32	2794	23	96
11A587.D	6.257	0.071	0.365	0.0038	2005	18	2015	13	100
11A588.D	7.11	0.086	0.3908	0.0045	2126	21	2113	18	101
11A589.D	5.217	0.056	0.3324	0.0037	1849	18	1852	17	100
11A590.D	6.892	0.065	0.3818	0.0041	2084	19	2101	15	99
11A591.D	13.62	0.21	0.53	0.0071	2742	29	2705	20	101
11A592.D	5.81	0.081	0.3621	0.004	1991	19	1894	20	105
11A594.D	7.27	0.12	0.3935	0.0063	2137	29	2125	18	101
11A595.D	5.236	0.055	0.3363	0.0032	1868	15	1832	14	102
11A596.D	7.313	0.077	0.3971	0.0043	2155	20	2150	15	100
11A601.D	6.107	0.083	0.3726	0.0047	2040	22	1930	21	106
11A602.D	6.375	0.068	0.3779	0.0041	2067	19	1984	13	104
11A603.D	5.14	0.063	0.3354	0.0044	1863	21	1823	20	102
11A604.D	8.96	0.19	0.438	0.0065	2340	29	2325	20	101
11A605.D	7.22	0.11	0.3944	0.0054	2142	25	2119	22	101
11A606.D	5.278	0.07	0.3366	0.0039	1869	19	1861	19	100
11A607.D	5.533	0.071	0.3448	0.0038	1909	18	1888	16	101
11A608.D	5.869	0.078	0.3554	0.0045	1959	21	1939	22	101
11A609.D	5.682	0.07	0.3481	0.004	1925	19	1931	17	100
11A610.D	9.61	0.13	0.4414	0.0055	2355	24	2440	19	97
11A611.D	4.972	0.059	0.3297	0.0038	1836	19	1787	20	103
11A612.D	7.481	0.094	0.3952	0.005	2146	23	2187	19	98
11A613.D	10.95	0.16	0.458	0.0081	2429	36	2569	22	95
11A614.D	8.39	0.11	0.4179	0.0048	2252	22	2295	16	98
11A615.D	6.819	0.095	0.3879	0.0052	2111	24	2056	18	103
11A616.D	7.64	0.11	0.4163	0.0052	2242	24	2141	25	105
11A617.D	8.41	0.17	0.4241	0.0078	2279	35	2285	15	100
11A618.D	12.69	0.22	0.5082	0.0084	2654	36	2656	29	100
11A619.D	5.723	0.065	0.3533	0.0037	1951	18	1913	14	102
11A620.D	8.911	0.096	0.4338	0.0056	2324	25	2315	16	100
11A621.D	4.977	0.061	0.3254	0.0037	1815	18	1800	22	101
11A622.D	5.291	0.056	0.3362	0.0035	1871	17	1850	18	101
11A623.D	5.202	0.062	0.3364	0.0036	1869	17	1824	17	102
11A624.D	8.96	0.1	0.4372	0.0047	2337	21	2326	15	100
11A625.D	5.61	0.13	0.3527	0.0059	1948	29	1879	29	104
11A626.D	7.832	0.075	0.417	0.0041	2246	18	2171	14	103
11A627.D	10.61	0.13	0.4682	0.0055	2478	24	2496	18	99
11A628.D	7.73	0.12	0.4092	0.0058	2210	27	2157	19	102
11A629.D	10.84	0.19	0.4595	0.0071	2440	32	2529	20	96
11A630.D	10.45	0.12	0.4629	0.0055	2453	24	2497	20	98

11A631.D	8.42	0.12	0.4165	0.0045	2243	20	2303	17	97
11A632.D	5.81	0.072	0.3562	0.0038	1966	18	1925	16	102
11A633.D	5.317	0.076	0.3401	0.0044	1888	21	1852	22	102